

QUANTIFYING THE GLACIAL MELTWATER COMPONENT OF
STREAMFLOW IN THE MIDDLE FORK NOOKSACK RIVER,
WHATCOM COUNTY, WA, USING A DISTRIBUTED
HYDROLOGY MODEL

BY

Carrie B Donnell

Accepted in Partial Completion
of the Requirements for the Degree
Master of Science

Moheb A Ghali, Dean of Graduate School

ADVISORY COMMITTEE

Chair, Dr. Robert Mitchell

Dr. Doug Clark

Joanne Greenberg, P.E.

MASTER'S THESIS

In presenting this thesis in partial fulfillment of the requirements for a master's degree at Western Washington University, I agree that the Library shall make its copies freely available for inspection. I further agree that extensive copying of this thesis is allowable only for scholarly purposes. It is understood, however, that any copying or publication of this thesis for commercial purposes, or for financial gain, shall not be allowed without my written permission.

Signature _____

Date _____

QUANTIFYING THE GLACIAL MELTWATER COMPONENT OF
STREAMFLOW IN THE MIDDLE FORK NOOKSACK RIVER,
WHATCOM COUNTY, WA, USING A DISTRIBUTED
HYDROLOGY MODEL

A Thesis
Presented to
The Faculty of
Western Washington University

In Partial Fulfillment
of the Requirements for the Degree
Master of Science

by
Carrie B Donnell
March 2007

ABSTRACT

Glacial meltwater is a vital component of rivers and streams in glaciated regions such as the Pacific Northwest, and can be critical for municipal water supplies, power generation, and habitat issues. The Middle Fork of the Nooksack River is fed by meltwater from Deming Glacier on Mount Baker, WA. The City of Bellingham has been diverting water from the Middle Fork since 1962 to supplement the water supply, and to maintain water quality in Lake Whatcom, the water source for the city. Because of regulations, water is only diverted when the Middle Fork exceeds minimum acceptable streamflow. A concern for water resource managers in Whatcom County, WA, is that Deming Glacier is retreating. In this study, the Distributed Hydrology Soils Vegetation Model (DHSVM) is used to perform a detailed assessment of the hydrology in the Middle Fork basin, to quantify future meltwater contributions to the Middle Fork Nooksack River as Deming Glacier continues to retreat, and to evaluate streamflow contributions based on predicted climate change.

DHSVM is a physically based, spatially distributed hydrology model that simulates a water and energy balance at the pixel scale of a digital elevation model (DEM). DHSVM requires multiple GIS input grids to characterize the watershed including a DEM, soil type, soil thickness, vegetation, stream network, and watershed boundary. Required meteorological input includes an hourly time series of air temperature, relative humidity, incoming shortwave and longwave radiation, and wind speed. Meteorological data were compiled from historical records of lower-altitude weather stations. The model was calibrated to measured snow-water equivalent at the Middle Fork SNOTEL station and stream discharge at the USGS stream gauge on the Middle Fork using a 1-hour time step and

50 m GIS grid resolution. Once calibrated, the model was applied to examine the effects of glacier size on streamflow. The model was also applied to simulate future streamflow based on predicted future climate change scenarios.

The estimated glacial meltwater component of late-summer streamflow as defined by the 2002 glacier coverage and present climate conditions was between 8.4% and 26.1%, depending on the climate of a given year (wet year vs. dry year). The late-summer glacial meltwater component was greater for drought simulations and predicted climate simulations, but less for increased precipitation simulations. DHSVM consistently simulated a smaller glacial meltwater component for progressively smaller glaciers. Simulation results suggest that late-summer streamflow in the Middle Fork could be reduced by as much as 8.6% as the direct result of glacier shrinkage predicted in the next fifty years, or by as much as 15.7% as the result of glacier shrinkage *and* predicted climate change for the same time period.

Glacier shrinkage could have significant implications for salmon habitat and migration during the late-summer, and may in turn compromise the feasibility of the Middle Fork Nooksack diversion. Further research is necessary to evaluate the effects of glacier shrinkage on the entire Nooksack watershed, particularly the North Fork.

ACKNOWLEDGEMENTS

First and foremost, I would like to thank my thesis committee for all of the help and insight they provided me throughout the research process. Bob Mitchell, Doug Clark, and Joanne Greenberg comprised a very well rounded committee. I would also like to thank Katie Kelleher and Jay Chennault for always being willing to answer DHSVM questions. Mike Johnsen was an invaluable asset, as he helped me through many GIS problems. Niki Bowerman helped with field work and lab analysis. Finally, I would like to thank Kelsay Davis for housing me on my many trips back to Bellingham.

TABLE OF CONTENTS

ABSTRACT	iv
ACKNOWLEDGEMENTS	vi
TABLE OF CONTENTS	vii
LIST OF TABLES	ix
LIST OF FIGURES	x
1.0 INTRODUCTION	1
2.0 BACKGROUND	3
2.1 Middle Fork Nooksack Watershed	3
2.1.1 Middle Fork Nooksack River	3
2.1.2 Geologic setting	4
2.1.3 Glaciers	4
2.1.4 Soils	6
2.1.5 Vegetation	7
2.1.6 Climate	7
2.2 Previous work	8
2.2.1 Mass balance studies	8
2.2.2 Runoff studies	11
2.2.3 DHSVM studies	13
3.0 RESEARCH OBJECTIVES	14
4.0 METHODS	14
4.1 Basin setup	15
4.1.1 DEM	15
4.1.2 Watershed boundary	15
4.1.3 Landcover	16
4.1.4 Soil classifications	16
4.1.5 Soil thickness	16
4.1.6 Stream network	17
4.2 Meteorological data	17
4.3 Streamflow and diversion data	19
4.4 Calibration and validation	20
4.4.1 Calibration	20
4.4.2 Validation	23
4.5 Simulating glacial melt	23
4.6 Glacial melt experiments	26
4.6.1 Present climate and different glacier coverages	27
4.6.2 Drought and increased precipitation scenarios	30
4.6.3 Predicted climate change for the Pacific Northwest	30
5.0 RESULTS AND DISCUSSION	31
5.1 Basin setup	32
5.2 Meteorological data	32
5.3 Calibration and validation	33
5.3.1 Calibration	33
5.3.2 Validation and potential errors	36

5.4 Glacial melt experiments	40
5.4.1 Present climate and different glacier coverages	40
5.4.2 Drought scenario and 2002 glacier coverage.....	45
5.4.3 Increased precipitation scenario and 2002 glacier coverage	48
5.4.4 Predicted climate scenario with 2002 and predicted 2050 glacier coverages	50
5.4.5 Summary of glacial melt experiments	52
5.5 Implications	54
6.0 CONCLUSIONS	54
7.0 FUTURE WORK	57
8.0 REFERENCES	58
APPENDIX A: DHSVM basin setup	89
APPENDIX B: Table of all calibration and validation simulations performed	99
APPENDIX C: Contents of disc	103

LIST OF TABLES

Table 1: Monthly precipitation sums and average air temperature for meteorological input files (SNOTEL and synthetic) and Clearbrook weather station	62
Table 2: Vegetation hydrologic parameters	63
Table 3: Soil hydrologic parameters	63
Table 4: Location of SNOTEL, weather, and stream gauging stations	64
Table 5: Glacier coverage in the Middle Fork Basin for discrete time periods	64
Table 6: Measured and simulated snow-water equivalent at the Middle Fork SNOTEL station	65
Table 7: Contribution of glacial meltwater to streamflow in the Middle Fork Nooksack River using present meteorological conditions (WY 2003-2005) and different glacier sizes	66
Table 8: Change in glacier melt using present meteorological conditions and different glacier sizes	67
Table 9: Change in total stream discharge using present meteorological conditions and different glacier sizes	68
Table 10: Glacial meltwater component of streamflow for drought scenario and 2002 glacier coverage	69
Table 11: Change in glacier melt compared to present meteorological and glacier conditions	69
Table 12: Change in total stream discharge for drought scenario and 2002 glacier coverage	69
Table 13: Glacial meltwater component of streamflow for increased precipitation scenario and 2002 glacier coverage	70
Table 14: Change in glacier melt compared to present meteorological and glacier conditions	70
Table 15: Change in total stream discharge for increased precipitation scenario with 2002 glacier coverage	70
Table 16: Glacial meltwater component of streamflow for predicted climate scenario with 2002 and predicted 2050 glacier coverage	71
Table 17: Glacier discharge for predicted climate scenario with 2002 and predicted 2050 glacier sizes	71
Table 18: Change in total stream discharge for predicted climate scenario with 2002 and predicted 2050 glacier sizes	72
Table B1: Table of all calibration simulations performed using three meteorological stations	99
Table B2: Table of all calibration simulations performed using Elbow Lake Meteorological station	99
Table B3: Table of all calibration simulations performed using Middle Fork meteorological station	100

LIST OF FIGURES

Figure 1: Location of Middle Fork Nooksack watershed and associated stream gauges and SNOTEL sites	73
Figure 2: Conceptual model of DHSVM.....	74
Figure 3: DEM of Middle Fork Nooksack watershed	74
Figure 4: 2002 vegetation grid of Middle Fork Nooksack watershed.....	75
Figure 5: Soil classifications in the Middle Fork Nooksack watershed	75
Figure 6: Soil thickness in Middle Fork Nooksack watershed	76
Figure 7: Stream network in Middle Fork Nooksack watershed.....	76
Figure 8: 17% glacier size reduction (predicted for year 2050).....	77
Figure 9: 48% glacier size reduction (predicted for year 2150).....	77
Figure 10: 0% Glacier coverage	78
Figure 11: 144% glacier size increase (estimated for LIA).....	78
Figure 12: Location and ages of wood samples for radiocarbon dating.....	79
Figure 13: First calibration simulation with default parameters.....	80
Figure 14: Mean monthly stream discharge with different soil thickness.....	80
Figure 15: Mean monthly stream discharge with different precipitation lapse rates.....	81
Figure 16: Mean monthly stream discharge with different temperature lapse rates	81
Figure 17: Stream hydrograph before calibrating to snow-water equivalent	82
Figure 18: Simulated and measured snow-water equivalent at Middle Fork SNOTEL site	82
Figure 19: Stream hydrograph for calibrated model WY 2005.....	83
Figure 20: Stream hydrograph for validated model for WY 2003	83
Figure 21: Stream hydrograph for validated model for WY 2004	84
Figure 22: Total stream discharge for calibration and validation periods.....	84
Figure 23: Glacial meltwater contribution for WY 2003 and 2002 glacier coverage	85
Figure 24: Glacial meltwater contribution for WY 2003 and 2050 glacier coverage	85
Figure 25: Glacial meltwater contribution for WY 2003 and 2150 glacier coverage	86
Figure 26: Glacial meltwater contribution for WY 2003 and LIA glacier coverage	86
Figure 27: Stream discharge for WY 2003 and all glacier sizes	87
Figure 28: Snow-water equivalent for water years 2003-2005 at Middle Fork SNOTEL ...	87
Figure 29: Summary of melt experiments	88

1.0 INTRODUCTION

Glaciers in Washington's North Cascades are a vital hydrologic resource because they store a significant volume of frozen water and they tend to moderate discharge in glacier-fed streams. Specifically, glaciers store excess precipitation during wet winters, whereas increased melting during warm, dry periods produces more runoff, thus damping the seasonal fluctuations of runoff in a stream (Fountain and Tangborn, 1985). In the same manner, glaciers buffer the effects of regional droughts. The volume of runoff from a glacier is primarily a function of glacier area. Consequently, smaller glaciers do not produce as much runoff as larger glaciers (Rango et al., 1979). Understanding regional glaciers is therefore essential for water resources management.

A concern for water resource managers in Whatcom County, Washington, is that Deming Glacier has been retreating during the past century. The Middle Fork of the Nooksack River is fed by meltwater from Deming Glacier on Mount Baker (Figure 1). The City of Bellingham has been diverting water from the Middle Fork since 1962 in order to supplement the supply of water to Lake Whatcom, the water source for the city (Walker, 1995; Figure 1). Also, the flushing effect of the diverted water may help maintain the overall water quality in Lake Whatcom (Walker, 1995). The diverted water may account for up to 80% of the surface inflow into Lake Whatcom during the summer and 20% of the city's yearly water consumption (Tracy, 2001). As Bellingham continues to grow, so will its water needs.

By law, the city must maintain the legal water level of Lake Whatcom below 314.94 ft above mean sea level (AMSL) and is allowed no more than a four foot fluctuation below that level (Ecology, 1985). The Instream Resources Protection Program (IRPP)

stipulates that water can only be diverted to Lake Whatcom when flow in the Middle Fork exceeds 275 cubic feet per second (cfs) in most months, the minimum necessary streamflow for salmon migration (Ecology, 1985). Diversion cannot occur in June and half of July unless streamflow exceeds 525 cfs (J. Greenberg, personal communication). As the surface area of Deming Glacier decreases, summer streamflow will likely decrease in the Middle Fork (Pelto, 2003). Therefore, a quantitative assessment of the influence of Deming glacier on streamflow in the Middle Fork is necessary for future water resource planning in Whatcom County, WA. I performed this assessment using hydrologic simulation modeling.

Hydrologic simulation modeling began in the 1950s and 1960s with the introduction of the digital computer. The primary focus of modeling at the time was streamflow forecasting, design and planning for flood protection, and extension of streamflow records (Storck et al., 1998). Early models were spatially “lumped,” meaning that heterogeneities of a basin were not modeled explicitly, but the effective response of an entire watershed was characterized. Although spatially lumped models are still in wide use today, they do not represent the spatial variability of hydrological processes and watershed parameters (Storck et al., 1998). The development of spatially distributed models in the last ten years has been made possible by the availability of detailed land surface data as well as the rapid increase in desktop computing power. Distributed models have many important applications for the interpretation and prediction of potential effects of land use change on watershed characteristics (Storck et al., 1998).

The Distributed Hydrology Soils Vegetation Model (DHSVM) was developed at the University of Washington and Pacific Northwest National Laboratory and is one of the most sophisticated hydrologic models available (Wigmosta et al., 1994). The model simulates a

water and energy balance at the pixel scale of a digital elevation model (DEM; Figure 2). It has been applied predominantly to mountainous watersheds in the Pacific Northwest to simulate hydrologic responses to weather and land use conditions (e.g., Bowling and Lettenmaier, 2001; Chennault, 2004; Storck et al., 1995, 1998; Wigmosta and Perkins, 2001). Required input for DHSVM includes a DEM, watershed boundary, soil classifications, soil depth, vegetation classifications, stream flow data, and meteorological data.

I applied DHSVM to quantify present and future meltwater contributions to the Middle Fork Nooksack River as Deming Glacier continues to retreat at the historic rate, and under a variety of climatic conditions. This assessment provides a quantitative evaluation of the relationship between glacier size and runoff, which will aid researchers in evaluating the responses of other alpine stream systems to changes in glacier size.

2.0 BACKGROUND

In order to model streamflow in the Nooksack drainage basin, classification of the local topography, geology, glaciers, soils, vegetation, and climate is essential, as these parameters are required input for DHSVM.

2.1 Middle Fork Nooksack watershed

2.1.1 Middle Fork Nooksack River

The main stem of the Nooksack River occupies a valley of thick alluvium with an approximate average gradient of 12 m/km for most of its length. The Nooksack has three

main tributaries including the North, Middle, and South Forks which all converge near Deming, WA (Figure 1). The Middle Fork is the focus of this study.

The gradient of the Middle Fork is variable, ranging from 71 m/km upstream to 13 m/km near its confluence with the North Fork. The headwaters of the Middle Fork originate at Deming Glacier (Figure 1). The area of the Middle Fork watershed is approximately 260 km².

2.1.2 Geologic setting

The Middle Fork basin is located on the southwest flank of Mt. Baker, WA. Mt. Baker is an active volcano located approximately 53 km east of Bellingham, WA and 24 km south of the Canadian Border in the Cascade Range. It is the highest peak in the north Cascades and is one of a cluster of volcanoes that make up a Quaternary volcanic field. The modern dome which is less than 30,000 years old overlies the remnants of Black Buttes volcano, an older volcanic dome that was active approximately 300,000 to 500,000 years ago (Gardner et al., 1995).

2.1.3 Glaciers

Mt. Baker is the second most heavily glaciated volcano in the Cascades (second only to Mt. Rainier) and is largely covered by 1.8 km³ of snow and ice 1800 m AMSL (Gardner et al., 1995). During the late Pleistocene, thick ice related to the advance of the Cordilleran ice sheet filled valleys and covered the region up to ~1300 m AMSL (Gardner et al., 1995). Although much of the ice in the surrounding area melted at the close of the Pleistocene, Mt. Baker remains heavily glaciated. Ten major glaciers terminate between 1200 m and 1800 m

AMSL on Mt. Baker (Harper, 1992). The glaciers are drained radially by tributaries of the Nooksack River and the Baker river branch of the Skagit River.

Deming Glacier is a southwest oriented temperate valley glacier that dominates the headwaters of the Middle Fork basin. The source of accumulation for Deming Glacier is direct snowfall with minor drift snow (Post et al., 1971). As of 1980, the glacier measured approximately 4.8 km in length and 4.5 km² in area (Fuller, 1980). These measurements overestimate present glacier size, however, because the glacier has retreated since 1980. The width of Deming Glacier is variable; it has a wide accumulation zone and a narrow terminal tongue. The head elevation of Deming Glacier is 3260 m AMSL and the terminus is confined by steep valley walls at approximately 1340 m AMSL. The majority of the glacier's mass is located between 2,000 m and 2,500 m AMSL. The average surface slope of Deming Glacier is 19.6° (Post et al., 1971). Deming glacier is heavily crevassed, has an ice fall between 1645 m and 1825 m, and terminates on a moderate to low slope. As a result of the low surface slope near its terminus and relatively large area, Deming Glacier is likely the thickest glacier on Mt. Baker (Harper, 1992).

Although Deming Glacier is the dominant glacier in the Middle Fork basin, it is important to note that it is not the only glacier in the basin. Portions of the Twin Sisters Glaciers and Thunder Glacier also feed into the basin. Although the modern meltwater contribution to the Middle Fork from the latter glaciers may be small, it is nonetheless present, and likely had more influence on streamflow in the past when those glaciers were larger.

After retreating significantly early in the 20th Century, Deming Glacier advanced beginning in the 1950s, then began retreating again in 1987. Between 1987 and 2002, the

glacier retreated approximately 360 m (Pelto, 2003). Retreat will likely continue into the foreseeable future. However, because the glacier is so thick, it will probably continue to retreat at a slow, steady pace (Pelto, 2003).

Historic glacier inventories help to characterize the recent behavior of Deming Glacier. The first comprehensive glacier inventory in the North Cascades that includes Mt. Baker glaciers was completed by Post et al. (1971). The inventory was based on aerial photos that were taken in the 1950s. The report includes 756 glaciers having a combined area of 267 km². Post et al. (1971) also included analyses of the hydrologic significance and spatial characteristics of the glaciers.

A more recent glacier inventory has been completed in the North Cascades National Park Complex by Frank Granshaw (2002) of Portland State University. Granshaw's inventory was based on aerial photos from 1998. He digitized his inventory of 1998 glaciers as well as Post's (1971) 1950s glaciers into a Geographical Information System (GIS). The more recent inventory does not include Deming Glacier because it is not included in North Cascades National Park, but it is useful nonetheless for examining regional glacier behavior between the 1950s and 1998. Granshaw (2002) noted an average of 7% area loss throughout the complex since 1958.

2.1.4 Soils

Two dominant types of soil occur in the Middle Fork basin (Goldin, 1992). The first is loam that was formed in either a mixture of volcanic ash and loess over glacial outwash or colluvium derived from glacial till. The colluvium is derived dominantly from dunite. The

second soil type is riverwash that is formed on land that is frequently flooded. Minor gravelly loam also occurs in the area (Goldin, 1992).

2.1.5 Vegetation

Three broad regions of vegetation occur within the North Cascades including a Tsuga Heterophylla (Western Hemlock) zone, subalpine zone, and timberline or alpine zone (Goldin, 1992; Franklin and Dyrness, 1973). The first zone consists mainly of Western Hemlock, Douglas Fir, and Western Red Cedar. The subalpine forest consists mainly of Cascades Fir, Alpine Fir and Mountain Hemlock. Other vegetation in the area includes salal, red huckleberry and Western sword fern. The alpine zone is heavily glaciated or has been recently deglaciated and is being revegetated.

2.1.6 Climate

Climate in the area of the Middle Fork can be highly variable, but is typified by warm, dry summers and cool, wet winters (see the 75-year monthly average temperature and precipitation for the Clearbrook weather station in Table 1; Figure 1). Regional climate is controlled by the interaction between meteorological conditions produced by atmospheric pressure patterns and local topography. Maximum precipitation occurs in the winter and minimum precipitation occurs during mid-summer (Fountain and Tangborn, 1985). Precipitation generally increases with elevation while temperature generally decreases with elevation in the study region.

Peaks reaching 1500 m to 2000 m AMSL on the Olympic Peninsula and Vancouver Island tend to reduce the precipitation of storms moving into the North Cascades. The

Straight of Juan De Fuca and the Straight of Georgia, on the other hand, act to funnel westerly storms into the region (Harper, 1992). The Cascade Mountains orographically block weather related to the Washington interior, thus isolating western Washington from the warmer summer temperatures and colder winter temperatures found east of the crest.

2.2 Previous work

Hydrologic modeling is one of a variety of methods that can be used to estimate glacier meltwater input to streams. Mass balance measurements, meteorological data and streamflow analyses have also been used to estimate glacial meltwater.

2.2.1 Mass balance studies

Mass balance measurements have been used regionally to estimate glacier meltwater contributions to mountain streams in the North Cascades as well as to determine the rate at which North Cascades glaciers are receding. Glaciers are sensitive indicators of climate change; they continually preserve a record of meteorological information in remote locations spanning great periods of time. Glacier annual mass balance is the most sensitive indicator of a glacier's response to changes in climate. The mass balance of glaciers in any mountain range varies due to local meteorological complexities and variation in aspect and hypsometry. It is therefore necessary to study a large number of glaciers in a mountain range to understand the overall trend in mass balance of glaciers in the region (Pelto, 1996). No detailed mass balance measurements have been made on Deming Glacier. However, several glacier mass balance studies have been conducted across the region during the past two decades (Pelto, 1996; Reidel et al, 1999).

In 1997 the USGS proposed a three-tiered program to improve glacier monitoring in the northwest in a cost-effective way. Mass balance studies can be very expensive, and the cost of a regional monitoring program is greatly reduced by intensively monitoring only a few glaciers and using the data to estimate regional glacier change. Tier-1 glacier monitoring includes detailed surface measurements of mass balance, meteorological data and water runoff whereas tier-2 glacier monitoring is limited to measures of annual mass balance using a two-season mass balance measuring approach (Fountain et al, 1997). Tier-3 glacier monitoring utilizes remote sensing techniques to define changes in snow and/or ice areal extent. USGS estimates have also been compared to less detailed glacier mass balance measurements for the entire region (Pelto and Riedel, 2001).

The most intensively monitored glacier in the region is South Cascades Glacier (a tier-1 glacier). The USGS has been monitoring South Cascade Glacier annually since 1958. It was selected for detailed study based on its similarity to other glaciers in the region, ease of access, and extent of previous mass balance measurements. It has been noted by researchers for the North Cascades National Park, however, that the South Cascade Glacier is not representative of all glaciers in the Park, particularly those on the east-slope (Riedel et al., 1999). Tangborn et al. (1975) conducted a study comparing mass balance measurements of South Cascade Glacier using mapping, glaciological, and hydrological methods. The mapping and glaciological methods of estimating mass balance showed close comparison with each other (within 5%) and are considered reliable methods. The mass balance that was estimated using the hydrological method was 38% higher than that estimated using mapping or glaciological methods. The difference is most likely due to the release of stored liquid water in the summer (Tangborn et al., 1975).

Geologists from the North Cascades National Park have been monitoring four tier-2 glaciers in the North Cascades since 1993 (Riedel et al, 1999). Noisy Creek, Silver, North Klawatti, and Sandalee Glaciers were chosen for study because of their geography, aspect, elevation, shape, and safety and ease of access. The main goals of the study are to monitor annual variation of the four glaciers, to examine variation at several time scales, to determine how well glaciers in the region are represented by South Cascade Glacier, and to aid in development of a system to monitor all glaciers in the North Cascades National Park (Riedel et al, 1999).

Additional mass balance monitoring is conducted as part of the North Cascades Glacier Climate Project (NCGCP), which was founded by Mauri Pelto in 1984 with the purpose of examining the response of glaciers to climate change (Pelto, 2001). The NCGCP has monitored the annual mass balance of at least eight glaciers since it was founded. Accumulation is measured using snow stratigraphy and probing methods in early summer, late July, and at the end of September. Ablation is measured in July and August of each year using a minimum of six stakes on each glacier. Although an extensive mass balance study of Deming Glacier has not been conducted, the NCGCP has been monitoring annual mass balance of Easton and Rainbow Glaciers on Mt. Baker since 1990 and 1984, respectively. Although variability among mass balances of glaciers in the North Cascades exists, cross correlation has shown that all of the glaciers have exhibited similar first-order responses to changes in climate since 1984 (Pelto,1996).

Annual glacier mass balance has also been empirically modeled for glaciers in the North Cascades using observations of precipitation, temperature, and run-off at low elevation weather stations (Tangborn, 1980). Tangborn concluded that these meteorological

records can be used to estimate accumulation, ablation, and mass balance of glaciers in the North Cascades.

2.2.2 Runoff studies

Approximately 75% of the total volume of global fresh water is stored in the form of glacial ice (Meier, 1984). North Cascade glaciers alone supply approximately 8.0×10^8 m³ of runoff each summer, or approximately 25-30% of the region's total summer water supply (Pelto, 1991). Estimates that glacier area in the North Cascades will decline by up to 25% in the next 20 years indicate that continued warming may lead to a decrease in glacial meltwater of 35% (Pelto, 1991). The importance of glacier runoff is increasing as water uses and needs in Washington State become fully realized. Present issues include competition for in-stream and out-of-stream water allocation. Therefore, monitoring of the regions glaciers and glacier runoff is important for water resources management. Numerous glacier runoff studies have been conducted in the North Cascades. However, most of the studies are qualitative and fail to consider many of the important hydrologic attributes of a basin. Following is a discussion of several glacier runoff studies that have led to the development of the comprehensive hydrologic model that I used to quantify the glacier meltwater contribution to the Middle Fork Nooksack River.

Researchers have compared streamflow in two basins having similar precipitation characteristics and hydrologic attributes, with the exception that one basin is glaciated and the other is non-glaciated (e.g. Meier 1986; Fountain and Tangborn, 1985; Pelto, 1991; Krimmel, 1992). The major assumption made in this type of study is that the difference in runoff between the two basins can be attributed to glacial meltwater (Krimmel, 1992).

Glacierized and non-glacierized basins that were studied in the North Cascades were chosen based on area, altitude, and location. The results of the studies indicate that glaciers play a crucial role in the timing, volume, and quality of runoff in a basin. For example, streamflow in a basin with 20% glacier cover can be as much as 50% greater than in a non-glaciated basin during the summer period (Fountain and Tangborn, 1985). Although the studies produce runoff results that are considered satisfactory, they fail to account for a number of fundamental physical attributes of a basin as well as any heterogeneities between basins.

Researchers have also modeled streamflow in a basin based on estimates of snow/glacier melt (e.g. Rango et al., 1979; Martinec and Rango, 1986; Rango, 1988; and Arnold et al., 1996). Rango et al. (1979) attempted to improve streamflow forecasting in two California basins by examining the effect of snow covered area on runoff volume. Martinec and Rango (1986) developed the ‘Snowmelt Runoff Model’ which they considered to produce ‘acceptable’ streamflow results. Arnold et al. (1996) developed a 3-D distributed model that calculates spatial and temporal variations in energy-balance components and, therefore, the melting of small valley glaciers. The modeling results supported the previous concept that the most influential factor in melt-energy of a glacier is solar radiation, specifically short-wave radiation. All of these studies produced reasonable results but failed to account for many important hydrologic attributes of the basins such as soils, vegetation, and topography.

A study conducted by Pelto (2003) of the glacial meltwater contribution of Deming Glacier to the Middle Fork Nooksack River was based on mass balance measurements of Easton Glacier, precipitation records, and Middle Fork discharge measurements. Results of the study indicate that glacial meltwater can contribute up to 30% of the streamflow in the

Middle Fork during a dry summer season. Bach (2002) examined the snowmelt contribution to streamflow in the Nooksack River above the town of Deming, WA, and found that the snowmelt contribution to the watershed increased from about 25% to approximately 31% between the 1940s and 1990s. Overall stream discharge, however, did not significantly increase during this time. This suggests that precipitation levels and other hydrologic factors are decreasing at the same rate that the snow and glacier melt is increasing (Bach, 2002). As with the others, these studies did not account for many hydrologic attributes of the basin.

Chennault (2004) examined the effect of glacier areal extent on streamflow in the Thunder Creek basin, North Cascades National Park, Washington. He performed his study using DHSVM, which accounts for the important hydrologic attributes of the basin including soil and vegetation hydrologic parameters. Chennault examined the influence of glacier size on streamflow by altering the size of glaciers in the basin and performing numerous model simulations. Major conclusions of the study are as follows. Glacial meltwater contribution to streamflow is highly dependent on the amount of precipitation during a given year, and varied from 0.6% to 56.6% contribution during late-summer for the Thunder Creek basin. Warm and dry years typically correspond to the largest percentage of glacial meltwater in the stream, while the influence of the glaciers is dampened during cool and wet years (Chennault, 2004).

2.2.3 DHSVM studies

DHSVM was first validated for the Middle Fork Flathead River, MT (Wigmosta et al., 1994). The original purpose of the model was to reproduce seasonal stream hydrographs and to examine the effects of snow areal extent on streamflow during spring snowmelt. The

model has since been used to simulate rain-on-snow events (Storck et al., 1995), to examine effects of changing land use patterns on streamflow (e.g., Bowling and Lettenmaier, 2001; Storck et al., 1998; Wigmosta and Perkins, 2001; Kelleher, 2006), and to evaluate the effects of glacier area on stream flow in glacierized basins (Chennault, 2004).

3.0 RESEARCH OBJECTIVES

The objective of my research was to use DHSVM to evaluate the effects of glacial retreat and predicted climate change on the streamflow in the Middle Fork Nooksack River, Whatcom County, Washington. I calibrated the model to both measured snow-water equivalent (SWE) at the Middle Fork SNOTEL station and stream discharge at the USGS stream gauge on the Middle Fork (Figure 1). I applied the model to examine the glacial meltwater component of streamflow in the Middle Fork using several different glacier ice extents including Little Ice Age (LIA) maximum, present size, and “future conditions” in which the Deming Glacier has significantly shrunk. I also applied the model to examine the influence of various climate scenarios on the glacial meltwater contribution to streamflow.

4.0 METHODS

Following is a discussion of the methods used to complete data collection, model calibration and validation, and analysis. Meteorological data collection and GIS input grid generation were completed during fall, 2005. Data were formatted and input to the program during winter 2005-06. Model calibration and validation took place during summer and fall 2006. Glacial melt experiments and analysis took place during fall, 2006.

4.1 Basin setup

DHSVM requires five GIS input grids including a DEM, landcover, soil type, soil thickness, and stream network. All grids were clipped to the watershed boundary. Meteorological data are also a DHSVM input requirement. Meteorological data were collected from lower elevation climate stations (Figure 1). Historical streamflow records were used for calibration and validation of the model, and were collected from a gauge on the Middle Fork that is maintained by the USGS. Following is a brief description of the GIS input grids used by DHSVM. A detailed explanation of GIS methods is found in Appendix A.

4.1.1 DEM

The DEM characterizes the topography of a watershed and is the foundation on which the distributive parameters of DHSVM such as temperature, precipitation, and water flow direction are based (Storck et al., 1995). The DEM for my study area was compiled from eight 7.5 minute, 10 m DEM files including Deming, Canyon Lake, Goat Mountain, Mt. Baker, Acme, Cavanaugh Creek, Twin Sisters, and Baker Pass. I ‘merged’ the DEMs and resampled them to 50 m by 50 m grid resolution using ArcGIS9 (Appendix A). The DEM was then clipped to the watershed boundary (Figure 3).

4.1.2 Watershed boundary

The watershed boundary was derived from the DEM using the interactive ‘hydrology modeling’ tool in ArcGIS9 (Appendix A). The watershed grid includes all pixels that eventually drain into the Middle Fork and is used as a template for all GIS grids (Storck et

al., 1995). All GIS grids were clipped to the watershed boundary to ensure that all grids have the identical number of overlapping cells.

4.1.3 Landcover

The landcover grid was generated from a 2002 landcover grid file from the National Oceanic and Atmospheric Administration (NOAA; http://www.csc.noaa.gov/crs/lca/pacific_coast.html). I resampled the vegetation grid to 50 m by 50 m resolution and reclassified vegetation classes to the classification scheme used by DHSVM (Figure 4, Appendix A). DHSVM only uses the dominant overstory species in each pixel and each vegetation classification is assigned vegetation-dependent hydraulic parameters with the use of a look-up table (Storck et al., 1995; Table 2). Glaciers are part of the vegetation grid.

4.1.4 Soil classifications

The soil type grid was generated using the 2002 soil data set from the State Soil Geographic Database (STATSGO; Miller and White, 1998; Appendix A, Figure 5). DHSVM only uses the primary soil type/texture in a given cell, and all cells with the same soil type are assigned one set of soil-dependent hydraulic parameters from a lookup table that was indexed by class specifically for DHSVM (Storck et al., 1995, Table 3).

4.1.5 Soil thickness

Soil thickness data do not exist for the study area. To model soil thickness, I used an Arc Macro Language (AML) script that was written at the University of Washington to automate a number of GIS commands (Appendix A; Figure 6). The soil thickness AML uses

a simple regression that calculates deep soil depths on shallow slopes and areas of high flow accumulation given a minimum and maximum soil thickness (Chennault, 2004). This type of AML has been used before with DHSVM and has provided acceptable results.

4.1.6 Stream network

The stream network grid was created using an AML script that creates the stream network as a series of distinct but connected reaches, based on stream order (Appendix A; Figure 7). Each reach is assigned attributes such as channel width, depth, and roughness (Storck et al., 1998). Flow networks created with this method have provided acceptable results in similar basins.

4.2 Meteorological data

DHSVM models two-story interception and evapotranspiration, soil evaporation, infiltration, subsurface flow and runoff in a basin using a meteorological input file that includes hourly maximum temperature, precipitation, long and short wave radiation, wind speed, and relative humidity (Storck et al., 1995). All modeling is based on established hydrologic relationships (e.g., Darcy's law and the Penman-Monteith equation). Temperature is distributed over the basin vertically using either a constant lapse rate or a variable lapse rate that can be changed between any time-step. Precipitation can be distributed by a constant elevation lapse rate or by using a precipitation model. Incoming solar radiation is distributed using a series of shading maps derived from the DEM (Appendix A).

I compiled three meteorological data files using a combination of lower elevation SNOTEL sites including Elbow Lake, Wells Creek, and Middle Fork, and the North Shore weather station in the Lake Whatcom watershed, western Whatcom County, WA (Figure 1, Table 4). DHSVM interpolates meteorological data between observation stations (Storck et al., 1998).

I acquired hourly observed temperature, precipitation, and wind speed data from each SNOTEL site. I imported data for water years (WY) 2003-2005. A water year begins on October 1st of one year and ends on September 30th of the subsequent year (e.g., WY 2005 begins on October 1, 2004 and ends September 30, 2005). I imported all data into an Excel spreadsheet for formatting. The first step in formatting was to evaluate the occurrence of missing data during the five year period. A complete data set would have 8761 hours per year, (8762 for leap year 2004). I then inserted blank cells as place holders for missing data. Precipitation data were recorded as *accumulated* precipitation. Many of the hourly values required manipulation, as data obtained from SNOTEL sites were only verified at hour 0:00 each day. Because data were given as accumulation, precipitation values necessarily ascend chronologically from zero precipitation (Oct 1) to total precipitation (Sep 30) for a given year. I ensured that all data ascended from the value at time 0:00 one day to the value at time 0:00 the next day. DHSVM requires hourly data, so I simply calculated the difference between accumulated precipitation at any hour (t_0) from the accumulated precipitation the following hour (t_1).

Temperature data were reported as 'observed temperature' each hour. Cells with missing values were given a value of 9999.99. I plotted temperature for each data set and evaluated the occurrence of missing data. I calculated any missing temperature

measurements as the mean of the temperature in the two time-adjacent cells. Missing data was rarely more than a few hours at a time. Monthly average temperatures for the input files are summarized in Table 1.

Wind speed values were handled similar to temperature data. Wind speed values were plotted for each data set. Missing values were located and calculated as the mean of the values in the two time-adjacent cells. Because wind speed magnitudes at Wells Creek and Elbow Lake were suspiciously low, I opted to use data from the North Shore weather station in western Whatcom County because of its completeness and availability (Figure 1).

Solar radiation and relative humidity were not available at SNOTEL stations used in this study. Instead, I collected these data from the North Shore weather station in western Whatcom County (Figure 1). Longwave radiation is not collected. Dr. Robert Mitchell modeled hourly longwave radiation using measured shortwave radiation and weather data from the North Shore weather station. These data were then used for model calibration.

4.3 Streamflow and diversion data

Measured streamflow data were used for model calibration and validation. Data were obtained from a gauging station on the Middle Fork that has been maintained by the USGS since 1992. However, the USGS station is located downstream of the Middle Fork diversion (Figure 1), so I adjusted the USGS data using diversion records acquired from the City of Bellingham. Diversion data were most important during the summer months. At the time of model calibration, diversion data were only available to me for WY 2005 (Oct. 1, 2004 – Sep. 30, 2005), which then became the calibration period. Diversion records were kept every five minutes. I converted all data to a one-hour time-step by averaging the five

minute data for each hour. Diversion data were necessary to reconstruct natural flow in the Middle Fork; otherwise DHSVM would overestimate streamflow at the USGS gauging station during times when the diversion was on. Unfortunately, hourly diversion data were not available to me for the model validation period. To evaluate more rigorously how accurate the validation simulations were, I calculated the difference in error between calibrated streamflow compared to measured streamflow at the Middle Fork stream gauge before and after adjusting for the diversion; the difference was 1.9%.

4.4 Calibration and validation

DHSVM is written in ANSI-C and requires a UNIX or LINUX platform. I performed most simulations on a PC having dual 3 GHz processors and a Free BSD (UNIX) operating system. Midway through model simulations, I changed to an Ubuntu LINUX operating system. Switching to LINUX had no effect on model results. I calibrated the model to measured climate and streamflow data. Following is a discussion of calibration and validation methods.

4.4.1 Calibration

Calibration is the process whereby model input parameters are adjusted so that simulated streamflow produced by the model is similar to measured streamflow from the Middle Fork gauging station from a specific time interval, thus ensuring that the model is estimating streamflow as accurately as possible ($\pm 5\%$). Although DHSVM is a physically based model, calibration is necessary because uncertainty exists in many of the required input parameters (Storck et al., 1995). Calibration for this project required calibration of

simulated SWE to that measured at the Middle Fork SNOTEL station, and calibration of simulated stream discharge to that measured at the USGS gauging station.

The first step in calibration was setting initial conditions for the beginning of each simulation. The initial conditions include the distribution of snow and water in the soil layers, vegetation layers, and ground surface (Storck et al., 1998). To establish initial conditions, I began a DHSVM simulation with a dry watershed and ran the model using meteorological data from WY 2005. It is important to use an entire year of meteorological data to establish the initial conditions to account for both dry and saturated conditions in the model state. WY 2005 was an average precipitation year (Table 1). I chose meteorological data from WY 2005 to establish the initial conditions to reduce the bias of an exceptionally wet or dry year. The hydrologic conditions at the end of WY 2005 were then used as the initial conditions for all subsequent simulations.

DHSVM can distribute air temperature and precipitation in a variety of ways using lapse rates. The temperature lapse rate dictates the cooling of an air mass with an increase in altitude. Similarly, the precipitation lapse rate dictates the increase in precipitation with an increase in altitude as a result of adiabatic cooling of the air mass. The simplest distribution method is using constant temperature and precipitation lapse rates.

Alternatively, air temperature can be distributed over the basin using a variable temperature lapse rate, and precipitation can be distributed using the Parameter-elevation Regressions on Independent Slopes Model (PRISM) precipitation grids. It has been observed during many DHSVM calibration experiments that air temperature decreases with altitude at different rates throughout the year (dry vs. wet lapse rate). Typically, in the Pacific Northwest, lapse rates range from $-4^{\circ}\text{C}/\text{km}$ during the winter months to around $-9^{\circ}\text{C}/\text{km}$ during the summer

months (Chennault, 2004). Simulated results can depend to a large degree on the distribution methods that are used.

Shortwave solar radiation measurements are made at a point source, and DHSVM distributes the measurements with the use of monthly shading maps that are created using an ArcGIS AML script (Appendix A). The shading files differ according to the time of year, time of day, and the topography surrounding the point source. In this way, the amount of shading throughout the basin is accounted for, and DHSVM distributes short wave radiation values accordingly. Longwave radiation is distributed over the basin uniformly, but is adjusted with the use of skyview maps that are also created using an ArcGIS AML script (Appendix A). The skyview maps define the percentage of sky that is exposed to each pixel cell. Relative humidity and wind speed are distributed uniformly over the entire basin.

I chose to calibrate DHSVM to WY 2005 due to the availability of diversion data. The Middle Fork experienced a number of high peak events as well as low summer streamflow, which provided a good test for model calibration. During calibration, I generally altered one parameter per simulation to evaluate the effects of each parameter on streamflow. The parameters that I concentrated on were temperature and precipitation lapse rates, snow/rain threshold temperatures, soil lateral hydraulic conductivity, and soil thickness (Appendix B).

DHSVM output consists of 42 parameters, and can be defined at any pixel for any time period. The two model output parameters that I used for calibration were SWE in meters defined near the Middle Fork SNOTEL station, and hourly streamflow in cfs defined near the USGS stream gauging station (Figure 1, Table 4). Output files were in ASCII

format. I imported these files to my PC via Secure Shell (SSH), then imported them into Excel for analysis.

4.4.2 Validation

Validation is the process whereby a calibrated model is used to simulate measured streamflow using a meteorological input file from a time period not included in the calibration. The simulated and measured streamflow for that period are then compared as a last assurance that the basin characteristics were established in the calibration process. The validation period for this project was WYs 2003-2004, as the Middle Fork SNOTEL station has only been in operation since WY 2003. The model is considered validated if the comparison between simulated and measured baseflow, peak events, and stream response time are comparable to that for the calibration application. Although diversion data were not available for the validation time period, I still consider the model validated based on the requirements listed above, and the relatively minor effect of the diversion (see section 5.3.2). The diversion is most influential during the summer months, and does not affect peak streamflow or stream response times throughout most of the year.

4.5 Simulating glacial melt

The aim of calibration is to capture the hydraulic properties of the Middle Fork basin as accurately as possible. This includes the properties that control how and when snow accumulates throughout the year, and when snow and glaciers start and stop melting during the year.

To simulate streamflow in the Middle Fork basin, it is important to understand how DHSVM simulates glacier ice melt. Snow accumulation and melt are modeled with DHSVM using a two-layer energy and mass balance approach. The two layers are a thin surface layer and a lower pack layer. Each grid cell receives water in both liquid and solid forms (rain and snow) and the model determines the form of precipitation based on the air temperature. During melt, the temperature of the snowpack is assumed to be isothermal at 0°C (Chennault, 2004).

In DHSVM, the energy-balance components are used to simulate snowmelt, refreezing, and changes in the snowpack heat content (Wigmosta et al., 2002). The energy-balance components include: net radiation flux (shortwave and longwave), sensible heat flux, latent heat flux, energy flux given to snowpack via rain and snow, and energy flux via refreezing and/or melting. Energy exchange between the atmosphere and the snowpack takes place in the surface layer only. Energy exchange between the two snowpack layers occurs from percolation of water from the surface layer to the lower pack layer and via ice exchange. Energy exchange via conduction and diffusion between the layers is ignored. Measured (or estimated) shortwave radiation, longwave radiation, relative humidity, wind speed, precipitation, and air temperature, which are required input to DHSVM, are used to calculate many of the above energy components.

Mass-balance components are used to simulate snow accumulation and ablation, changes in snow-water equivalent, and water yield from the snowpack (Wigmosta et al., 2002). The snowpack is composed of two phases; water and ice. Mass balance components include the volume per unit area of liquid water and the water equivalent of ice. The atmosphere exchanges water vapor with the ice phase during non-melt periods and with the

liquid phase during melt periods (Wigmosta, 1994). Mass is removed from the ice phase and added to the liquid phase during melting. If the liquid phase exceeds the liquid water holding capacity of the thin surface layer, then excess water is drained into the pack layer (Wigmosta, 2002). Similarly, if the ice phase exceeds maximum thickness of the surface layer, then it is distributed to the pack layer.

Glacial melt can be simulated using one of two methods in DHSVM. Glaciers are modeled as an inexhaustible snowpack using the same two-layer mass and energy balance used to model snow melt. An inexhaustible snowpack contains an infinite supply of water. The first method is to define vegetation type 20 as 'Glacier' in the input file. When using this approach, the model maintains a SWE of 5 m for all cells defined as 'Glacier', and the SWE is re-set during times of glacial melt, ensuring that the glacier does not theoretically melt away during model simulation. The second method is to define vegetation type 20 as 'Ice' in the input file. The model does not maintain a specified SWE throughout the melt period for all cells defined as 'Ice'. For my study, I used the former method, defining vegetation type 20 as 'Glacier'.

Streamflow can be defined and evaluated at any pixel within the watershed. When performing glacial melt experiments, one option is to define streamflow near the terminus of the glacier to better capture the effects of the glacier alone. However, for this application, I chose to output streamflow at the USGS gauging station to be consistent with my calibration and validation experiments.

4.6 Glacial melt experiments

Multiple episodes of glacier advance and retreat between the 15th and 20th centuries have been identified by moraine mapping and dating on Mt. Baker (Harper, 1992). To evaluate the relationship between glacier size and runoff, I generated several vegetation grids representing different glacier coverages, both larger and smaller than the 2002 glacier coverage (Figures 8-10, Table 5). The model was then used to predict future stream flow contribution based on potential glacial retreat, and to examine historic streamflow based on the magnitude of Deming, Twin Sisters, and Thunder Glaciers at their maximum LIA extents.

In addition to evaluating the relationship between glacier size and runoff, I examined simulated glacier discharge and total stream discharge resulting from different climate scenarios. To account for the influence of climate change on glacier melt and total stream discharge, I performed experiments based on present climate conditions (WYs 2003-2005), and based on predicted and hypothetical climate conditions.

I performed the following experiments to evaluate the effects of glacier size and climate conditions on glacier melt and total stream discharge: 1) present climate conditions with different glacier coverages, 2) drought conditions with present glacier coverage, 3) increased precipitation conditions with present glacier coverage, and 4) predicted climate with present *and* predicted glacier coverage. Following is a discussion of the glacial melt experiments.

4.6.1 Present climate and different glacier coverages

I created vegetation/glacier grids representing glaciers larger (LIA) and smaller (future glaciers) than the present (2002) coverage. Smaller glaciers estimates were based on the historic retreat rate of Deming Glacier. I then performed model simulations to examine the relationship between glacier size and runoff with meteorological data for WYs 2003-2005 as input. Following is a discussion of the methods used to estimate the different glacier coverages and to quantify glacier melt.

Future glacier sizes

I first attempted to establish the retreat rate of Deming Glacier since the LIA using moraine mapping and radiocarbon dating of buried logs. LIA moraine mapping was performed with the help of Dr. Doug Clark using aerial photos, and was verified by field mapping. In the field, we located several logs that were buried in till upstream of and underneath a terminal moraine complex, which is near the LIA terminal position (K. Scott, personal communication). We collected four samples; two from the upstream location, and two from the downstream location (Figure 12). The ages of the logs represent times when the trees were killed by the advancing glacier. This in turn provides information about the extent and age of Deming Glacier during the Holocene. After collecting the log samples, I selected small slivers of wood from near the outer surface of each. This was done to ensure that the resulting dates were as representative of the time at which the tree died as possible. Initial sample preparation took place at Western Washington University following the standard procedures for Accelerator Mass Spectrometry (AMS) radiocarbon dating at Lawrence Livermore National Laboratory in Livermore, CA (Vogel, 1984).

The AMS analyses indicate that the log samples are surprisingly old ($2,960 \pm 30$ and $2,970 \pm 35$ radiocarbon years for the upstream samples, and $2,440 \pm 30$ and $2,205 \pm 30$ radiocarbon years for the downstream samples; Figure 12), and were not in fact related to LIA moraines. We interpreted this as an older moraine that was later overlain by the LIA moraine, with no evidence of a soil horizon between the two. Because the logs were from an older advance, they were not useful for determining a retreat rate between the LIA and present.

As an alternative method, I established the average linear retreat rate of Deming Glacier since its LIA maximum extent using glacier extent and age data from Fuller (1980). Using digital aerial photos overlain by the 2002 landcover grid in ArcGIS, I located the LIA terminus that Fuller mapped and used the ArcGIS measuring tool to determine the linear distance between the LIA terminus and 2002 terminus. Using Fuller's dates and the distance that I measured, the resulting retreat rate is 5.4 m/yr. I applied the linear retreat rate to create several GIS grids representing possible future glacier scenarios (Figures 8-10). The reoccupation of vegetation in recently deglaciated terrain is assumed to have a negligible effect on the hydrologic response of the watershed, and all deglaciated pixels were therefore modeled as the "Bare" vegetation class (Chennault, 2004). Appendix A details the GIS methods used to create these grids.

I apply a conservative (slower), constant retreat rate (from LIA max to present) as opposed to the recent rapid retreat rate (during the past 30 years) in order to avoid over-emphasizing effects of short-term climate variability. Other scenarios are certainly possible. The glacier grids that I created are based on a conservative retreat rate (5.4 m/yr), assuming continuous *linear* retreat, which integrates across several high-frequency episodes of

advance and retreat that have occurred between the glaciers' maximum LIA extent and now (Harper, 1992). This method is only a first-order attempt to predict future glacier behavior. A more detailed attempt to predict future glacier behavior is beyond the scope of this thesis.

LIA glacier sizes

I created a GIS vegetation grid representing a reconstruction of the LIA glacier extents with the help of Dr. Doug Clark (Figure 10). We used a stereo pair of aerial photos to map out LIA moraines for the Deming, Twin Sisters, and Thunder Glaciers. Although the LIA extent of the terminal tongue of Deming Glacier is fairly well constrained by well-defined terminal moraines and changes in tree size, the Twin Sisters and Thunder Glaciers have not been studied in as much detail. This is only a first-order approximation of the LIA maximum extent of Deming, Twin Sisters, and Thunder Glaciers. A more rigorous reconstruction is beyond the scope of this thesis.

Quantifying glacial melt

As mentioned above, many studies have compared two basins with similar hydrologic characteristics with the exception that one basin is glaciated and the other is not. The difference in streamflow in the two basins is assumed to be the direct result of glacial melt. In this way, glacial contribution to streamflow can be evaluated. The same concept applies to this application of DHSVM. To quantify the present glacial meltwater component of streamflow, I created a vegetation grid in which all grid cells previously defined as 'Glacier' were reclassified as 'Bare' (Figure 11). I then applied DHSVM to simulate streamflow in two basins having not only similar, but *identical* hydrologic properties with

the exception that one is glaciated and the other is not. This approach therefore has the potential for improved results compared to the side-by-side studies because it eliminates the uncertainties related to the variability between any two basins.

4.6.2 Drought and increased precipitation scenarios

I created the synthetic drought and increased precipitation input files using a compilation of the three years of meteorological data that were used for calibration and validation. I created the drought file by inputting the driest meteorological data for each month. For example, I chose the driest October out of the three years, followed by the driest November, and so on. I then copied this one year of dry climate four times, resulting in a five year input file of hypothetical drought conditions. I used the same method for the increased precipitation file, with the exception that all data were the wettest for each month.

The glacial meltwater component of streamflow was determined using the same method that was used for present climate conditions (glaciated vs. non-glaciated basin). Potential increase/decrease in streamflow was determined by comparing streamflow for the drought and increased precipitation scenarios to streamflow based on present climate conditions.

4.6.3 Predicted climate change for the Pacific Northwest

I created a three-year meteorological input file based on predicted climate change in the Pacific Northwest. The Climate Impacts Group out of the University of Washington has performed numerous model simulations and has reviewed model simulations from around the world for predicting local climate change (Climate Impacts Group, 2004). Based on

their synthesis of the results of these model simulations, I chose to use an average increase in temperature of 1.4°C (October-March) and 1.8°C (April-September) and an increase in precipitation of 5% (October-March) and a decrease in precipitation of 4% (April-September). Using these predictions, I simply modified the meteorological data sets that I used for calibration and validation, resulting in a three-year predicted meteorological input file.

The glacial meltwater component of streamflow was determined using the same method that was used for other climate conditions (glaciated vs. non-glaciated basin). Potential increase/decrease in streamflow was determined by comparing streamflow for the predicted climate scenario to streamflow based on present climate conditions.

5.0 RESULTS AND DISCUSSION

The majority of the effort put into this project was dedicated to data collection, GIS grid generation for basin set-up, and model calibration and validation. After the model was successfully calibrated, I applied the model to examine the contribution of glacial meltwater to streamflow in the Middle Fork Nooksack River based on a variety of scenarios including variable glacier coverage and present and predicted climate.

Final products of this thesis include: a calibrated and validated DHSVM model of the Middle Fork Nooksack River basin which will serve as a basis for future modeling of glaciers on Mt. Baker; quantified present glacial meltwater component of streamflow in the Middle Fork; and simulated streamflow based on predicted climate scenarios and present glacier coverage. Following is a discussion of the results of my work.

5.1 Basin setup

Basin setup included the generation of five GIS input grids that were clipped to the watershed boundary (Appendix A). The data used to create these grids were the most recent data available at the time of this thesis. However, as updated data become available, new GIS grids can be created which can easily be incorporated into the model. If the data are better, the simulations should better approximate observed conditions. This model can therefore serve as a basis for future modeling studies of the hydrology in the Middle Fork Nooksack basin.

5.2 Meteorological data

The data file that I created to represent the meteorology of the Middle Fork Nooksack basin is comprised of a three-year time series of precipitation and air temperature obtained from the Middle Fork SNOTEL station, and wind speed, long and shortwave radiation, and relative humidity from the North Shore climate station near Lake Whatcom in western Whatcom County, WA. One of the challenges of this project was due to the fact that the latter meteorological parameters are not recorded within or even near the Middle Fork basin. Precipitation and air temperature are the most influential factors in modeling the hydrology of the Middle Fork basin. Precipitation dictates discharge volume, while the air temperature determines whether precipitation falls as snow or rain. The other meteorological parameters primarily control the timing of runoff. It is more essential that the meteorological input file contains local precipitation and temperature data; however, it is desirable that the other parameters be recorded at a station nearer to the study area. Again, if

newer data become available in the future, they can easily be incorporated into the model framework that I have created.

5.3 Calibration and validation

Continuous streamflow, diversion, and meteorological data allowed for this calibrated and validated hydrologic model of the Middle Fork Nooksack basin to be created. To complete calibration and validation, I performed 56 model simulations. Combined, these simulations took approximately 80 hours of computer run-time. Following is a discussion of the results of these model simulations.

5.3.1 Calibration

The primary focus of this application of DHSVM was to calibrate simulated streamflow to streamflow measured at the USGS gauging station. A secondary, but equally important objective was to calibrate predicted SWE to that measured at the Middle Fork SNOTEL station. Calibration of SWE was completed to determine the appropriate rain and snow threshold temperatures. Calibration of the model to streamflow was then performed to isolate precipitation and temperature lapse rates, soil thickness, and soil lateral hydraulic conductivity. I generally examined the effect of altering one of the above parameters at a time. See Appendix B for a description of all simulations performed.

Meteorological stations

I first attempted model calibration using meteorological input files from Elbow Lake, Wells Creek, and Middle Fork SNOTEL sites. Calibration using this method proved to be

more complicated than anticipated. The Middle Fork SNOTEL station was installed with the intention of monitoring the Middle Fork basin (J. Greenberg, personal communication). For this reason, I decided that precipitation and temperature data from the Middle Fork station would best represent the meteorology in the basin. See Table 1 for a summary of temperature and precipitation values used as input, and Appendix B for a description of calibration simulations performed with three meteorological input files.

USGS Streamflow

I first performed a simulation using DHSVM default parameters (Figure 13). The model underestimated measured peaks and baseflow (-43 % error). To improve simulation results, the first parameter that I examined was soil thickness. I created a series of soil thickness grids representing soils ranging in thickness from 0.76-1.5 m, 1.0-2.5 m, and 1.0-3.5 m. I found that DHSVM was not particularly sensitive to soil thickness in the Middle Fork basin (Figure 14), but the model most accurately predicted late-summer stream discharge using soils ranging in thickness from 1.0-2.5 m. I also adjusted the lateral hydraulic conductivity (K_L) of the most prominent soil type in the basin and found that DHSVM was most accurate using K_L of 0.005 m/s.

During the calibration process, I discovered that DHSVM was particularly sensitive to precipitation lapse rate. Using the default lapse rate of 0.0010 m/m, the model greatly underestimated baseflow and storm-event peaks (Figures 13 and 15). DHSVM responded to an increase in precipitation lapse rate in a manner opposite of that which was expected. An increase in the precipitation lapse rate corresponded to a further *decrease* in baseflow and storm-event peaks. A possible explanation for this observation is that the Middle Fork

SNOTEL station is located at a high altitude relative to the Middle Fork basin (Table 4). Precipitation increases with an increase in altitude at the same rate that precipitation decreases with a decrease in altitude. Therefore, it is reasonable that an increase in the precipitation lapse rate at the high altitude SNOTEL station would correspond to an overall decrease in streamflow. In order to accurately simulate streamflow in the Middle Fork, I decreased the precipitation lapse rate by an order of magnitude (Figure 15).

I evaluated the influence of various temperature lapse rates to determine whether a constant or variable lapse rate was more appropriate for modeling streamflow in the Middle Fork. Temperature inversions are common in the Middle Fork basin, making it very difficult to establish a consistent temperature lapse rate (J. Greenberg, personal communication). I found that the most appropriate temperature lapse rate was variable and equal to -0.0060 °C/km for November through June, and -0.0090 °C/km for July through October (Figure 16). I used this variable temperature lapse rate for all subsequent simulations. Similar temperature lapse rates have been used to simulate streamflow in the Pacific Northwest (Chennault, 2004).

Snow-water equivalent

After establishing the appropriate soil thickness, lateral hydraulic conductivity, precipitation lapse rate, and temperature lapse rate, DHSVM was able to accurately simulate streamflow for the months October-May, but greatly underestimated summer streamflow (Figure 17). The model was not producing enough snowpack throughout the year. To address this problem, I evaluated the model's sensitivity to the snow and rain threshold temperatures in the basin. I then compared predicted SWE defined at the Middle Fork

SNOTEL station to that which was observed at the station (Figure 18, Table 6). DHSVM modeled an increase in SWE through the month of April. A decrease in SWE commences in May, as does measured SWE (Figure 18; Table 6). However, the modeled snow does not completely melt during the summer as it does at the Middle Fork SNOTEL station. DHSVM was best able to simulate SWE with a snow and rain threshold temperature of 4°C. Although this seems high, the subsequent simulations produced enough snow-pack that predicted summer streamflow matched closely with measured streamflow.

Using the above parameter values, the model was considered calibrated with a 2.1 % error between total simulated and total measured streamflow (Figure 19).

5.3.2 Validation and potential errors

Model validation is performed to ensure that the model can accurately simulate streamflow using meteorological data sets different from those used for calibration. I validated the model for the Middle Fork using meteorological data from WYs 2003 and 2004. Validation simulation results are shown as stream hydrographs compared to measured streamflow (Figures 20 and 21) and as bar graphs representing total annual stream discharge (Figure 22). As previously stated, for the calibration simulation, I compared simulated streamflow to measured streamflow both before and after adjusting for the diversion. I found that the model under-predicted streamflow by 2.1% when accounting for the diversion, and by 0.18% without accounting for the diversion. The error is increased when accounting for the diversion because the under-prediction of summer streamflow is even more exaggerated when diversion values are added back in to measured streamflow.

The model is considered validated based on similarity to calibration results, and ± 4 % error between measured and simulated streamflow (Figures 20 and 21). As with the calibration simulation, storm-event peaks are generally under-predicted (assuming that measured peaks are reasonable), while baseflows generally agree with measured streamflow. All simulations show a slight under-prediction of summer streamflow (Figures 20 and 21). The error for the WY 2004 validation simulation is higher as a result of the high measured summer peak flows. Although the model is considered calibrated and validated, it is important to consider several potential errors associated with both measured and simulated data, and possible explanations for discrepancies between the two. Following is a discussion of potential errors.

Measured Streamflow

Streamflow discharge records for the Middle Fork are considered by the USGS to be 'fair' to 'good', except for discharges above 4000 cfs which are considered 'poor' (USGS, 2005). Discharges greater than 3,800 cfs are not directly measured, but are estimated by extending the stage-discharge rating curve using indirect measurements of peak events. This in turn can lead to significant errors in peak discharge values above 4,000 cfs. Peak discharges greater than 4,000 cfs occur frequently for the Middle Fork Nooksack River (Figures 19-21).

Middle Fork SNOTEL snow-water equivalent

Errors may be associated with the instrumentation used to collect SWE, air temperature, and precipitation data at the Middle Fork SNOTEL station. Basic

instrumentation used by the Natural Resources Conservation Services (NRCS) includes a pressure sensing snow pillow, storage precipitation gage, and air temperature sensor. The pressure-sensing snow pillow is a rubber membrane that contains a liquid with a low freezing point. Weight of snow on the pillow controls the pressure of the liquid which is recorded via a pressure transducer (Dingman, 2002). Several factors may affect the accuracy and continuity of the measurements including: variability of the instrument's liquid density due to changes in air temperature and atmospheric pressure, ice layers within the snowpack which act to 'bridge' the snow from the instrument and may lead to an underestimation of snowpack, leakage of measurable precipitation, and unstable power sources. However, NRCS snow-water equivalent data are considered to be accurate to within 2.5 mm.

As mentioned previously, precipitation and air temperature are required input for DHSVM, and these data are used to simulate SWE in the basin. The most prevalent source of error associated with the precipitation gauge is the result of wind, leading to an underestimation of snowpack.

Simulated snow-water equivalent

Several possible sources of error exist in the assumptions made to simulate SWE within DHSVM. In order for DHSVM to produce enough snowpack throughout the year for this application, I was forced to increase the maximum temperature at which snow occurs, and increase the minimum temperature at which rain occurs in the Middle Fork basin to 4°C. This value is rather high and may not be realistic. It may also be unreasonable to assume that the rain/snow threshold temperature is constant throughout the year. In addition, the

snow water capacity is user-defined in DHSVM. I used the default setting of 0.30 (snowpack is 30% water), but this is not well constrained.

Simulated glacial melt

In order for snow to commence melting in DHSVM, the entire snowpack must be isothermal at 0°C as well as completely saturated (Chennault, 2004). Warming of the snowpack by infiltration is unrealistic when applying the two layer model to a glacier. However, this should not be a problem in this case because most North Cascades glaciers are believed to be at or near isothermal conditions (D. Clark, personal communication). The inexhaustible snowpack method for estimating glacial meltwater is only appropriate for short-term modeling because simulated glaciers continue to produce melt water under the right conditions while maintaining their original areal extent. DHSVM does not simulate glacial retreat, and is therefore not appropriate for long-term modeling (a time period in which a glacier retreats significantly).

Another factor to consider when simulating glacial meltwater is basal melting. DHSVM does not account for basal pressure melting, which may contribute up to 10% of glacial meltwater on average for temperate mountain glaciers (Benn and Evans, 1998). This may or may not significantly affect glacial melt estimations, but should be considered nonetheless.

Although many possible sources of error exist for both the measured and simulated data, it is important to note that a major assumption for this application of DHSVM is that the measured values are accurate, and it is therefore reasonable to calibrate the model to the measured values.

5.4 Glacial melt experiments

The primary purpose of this thesis was to quantify the present glacial meltwater component of streamflow in the Middle Fork Nooksack River and to examine the relationship between glacier size and glacier runoff. I conducted a series of model simulations to examine the influence of the glacial meltwater on overall streamflow in the Middle Fork under a variety of climatic conditions including present conditions (WYs 2003-2005), drought, increased precipitation, and predicted climate change. Following is a discussion of the results of each of these experiments.

5.4.1 Present climate and different glacier coverages

To quantify the present glacial meltwater component of streamflow in the Middle Fork Nooksack River, I applied DHSVM using the calibrated model, three years of meteorological data that were used for model calibration and validation (WYs 2003-2005), and the vegetation/glacier grid representing Deming, Twin Sisters, and Thunder Glaciers at their 2002 extent (3.1% glacier coverage, Table 5). I then applied DHSVM to simulate streamflow using the same parameters but using the vegetation/glacier grid representing 0% glacier coverage (Figure 11). The difference in streamflow between the two simulations is glacial meltwater (Figure 23). I proceeded to perform simulations using the same input files, but with vegetation grids representing different glacier coverages to examine the relationship between glacier size and runoff. I compared all simulated streamflow to that which was simulated using the 0% glacier coverage grid (Figures 23-26).

Glacial meltwater contributions to streamflow

The glacial meltwater component of streamflow with the 2002 glacier coverage varied depending on the climate of a given year, and ranged from 1.5% to 2.3% annual contribution, and 8.4% to 26.1% late-summer contribution (Table 7). A 17% reduction in glacier size (predicted for year 2050) corresponds to meltwater contribution between 0.8% and 1.3% annual contribution, and between 6.9% and 19.2% late-summer contribution (Table 7). A 48% reduction in glacier size (predicted for year 2150) corresponds to meltwater contribution between 0.2% and 0.4% annual contribution, and between 1.8% and 8.3% late-summer contribution (Table 7). A 144% increase in glacier size (estimated for LIA maximum extent) corresponds to meltwater contribution between 7.6% and 10.8% annual contribution, and between 27.5% and 56.8% late-summer contribution (Table 7).

The meltwater component of streamflow with the various glacier sizes consistently decreased relative to glacier size (Figure 27). The range in the glacial meltwater contribution to streamflow for the simulations above can be explained by the variability in temperature, precipitation, and SWE for the three years of meteorological data used as model input (Figure 28, Table 1). DHSVM consistently simulated the highest percent contribution of glacial meltwater using meteorological data from WY 2003, which was the driest of the three years (Precipitation = 2.4 m; Table 1). It also consistently simulated the lowest percent contribution using meteorological data from WY 2004 which had the most overall precipitation of the three years of input (Precipitation = 3.1 m; Table 1). This makes physical sense because overall input to the stream during a dry year is lower than that for a year with more precipitation. Therefore, the glaciers will have more of an effect during a dry year, while the effect will be dampened during a wet year. However, results were not

necessarily consistent on the sub-yearly basis, depending on the *distribution* of precipitation throughout each year (Figure 28, Table 1). For example, summer meltwater contribution was lowest for WY 2005 as the result of high summer precipitation (June and July) relative to WYs 2003 and 2004 (Table 1).

Among all glacial melt experiments, the highest percent contribution of glacial meltwater to streamflow occurs during late-summer, while the lowest occurs annually (Table 7). This is due to the seasonal distribution of precipitation (Table 1) and the fact that the glaciers only melt during the summer months. Also, overall input to the stream is lowest during late-summer when precipitation is low and most of the snow in the basin has already melted, thus compounding the glacial effect.

The glaciers with the largest surface area consistently began melting earliest in the year, whereas the glaciers with the smallest surface area began melting latest in the year (Figures 23-27, Table 7). Similarly, the larger glaciers continued melting later in the year than the smaller glaciers. This result can be explained by the fact that I have forced a larger glacier to exist at lower altitude under present climate conditions for these simulations. For example, the LIA glacier extends deeper in the valley and to a lower altitude than that which naturally occurs with present climate conditions. As a result, the glacier at the lower elevation (LIA glacier) begins melting earlier in the year than the modern glacier (2002 coverage) that exists under present climate conditions. Among the different glacier sizes, the date when melting begins varies from April 24th to July 23rd (Figures 23-27, Table 7). The latest dates that the variable glaciers stopped melting range from October 6th to November 7th (Table 7).

Results of the variable glacier simulations agree with previous studies (i.e., Chennault, 2004; Pelto 2003). Chennault (2004) found that larger glaciers contribute more to streamflow and begin to melt earlier in the season than smaller glaciers. He also found that the amount of precipitation during a given year greatly influences the degree to which a glacier affects overall streamflow. Pelto (2003) concluded that meltwater from the Deming Glacier could contribute up to 30% of streamflow in the Middle Fork Nooksack River during the late-summer. Similarly, results of my study indicate that during a dry year (WY 2003), glacial meltwater may contribute approximately 26% of late-summer streamflow.

Change in glacier discharge compared to 2002 glacier coverage

Using meteorological data for WYs 2003-2005 (the same used for model calibration and validation) and 2002 glacier coverage, cumulative simulated glacier discharge ranged from $6.95 \times 10^6 \text{ m}^3$ to $1.15 \times 10^7 \text{ m}^3$ (Table 8). After calculating the cumulative glacier discharge for each of the various glacier coverages, I compared the resulting discharge to that for 2002 glacier coverage. Following is a discussion of the results of the variable glacier simulations.

A 17% reduction in glacier size (predicted for year 2050) corresponds to a decrease in glacier discharge between 40.2% and 45.9% compared to 2002 glacier coverage. Similarly, a 48% reduction in glacier size (predicted for year 2150) corresponds to a decrease in glacier discharge between 82.7% and 87.3% (Table 8). Simulated data suggest that a 144% increase in glacier size and present climate conditions would result in an increase in glacial discharge between 347.1% and 435.3%. However, it must be noted that

the latter estimation is not realistic, as glaciers as large as those during the Little Ice Age could not exist under present climate conditions.

Change in stream discharge compared to 2002 glacier coverage

Because the City of Bellingham diverts water from the Middle Fork just below the USGS stream gauge, it is important to consider how the different glacier sizes affect overall streamflow, and not only glacier discharge. Cumulative stream discharge modeled at the USGS gauging station ranged from $4.18 \times 10^8 \text{ m}^3$ to $5.45 \times 10^8 \text{ m}^3$ for present climate conditions and 2002 glacier coverage (Table 9). Using results of model simulations, I calculated streamflow (defined at the USGS gauging station) for each of the various glacier scenarios and compared the results to that for 2002 glacier conditions. This manipulation was performed to examine how an increase or decrease in glacier size would affect total stream discharge for annual, summer, and late-summer time periods (Table 9).

A 17% reduction in glacier size (predicted for year 2050) corresponds to a decrease in annual cumulative stream discharge between 0.67% and 1.05% compared to 2002 glacier coverage. Similarly, a 48% reduction in glacier size (predicted for year 2150) corresponds to a decrease in annual stream discharge between 1.28% and 2.07% (Table 9). Simulated data suggest that a 144% increase in glacier size and present climate conditions would result in an increase in annual stream discharge between 6.67% and 9.46%. Again, the latter estimation is not realistic because the simulation was performed with LIA glacier coverage and present climate conditions. These two conditions can not exist in nature simultaneously.

The maximum decrease in annual and late-summer stream discharge consistently occurs with the water year 2003 meteorological input file for all glacier scenarios. This

observation can be explained by the fact that WY 2003 had the least precipitation (Table 1), and therefore it is the year that is most sensitive to a change in glacial meltwater input. The maximum difference in stream discharge consistently occurred during the late-summer (Table 9). Again, late-summer is when the glaciers significantly affect streamflow due to lower overall stream inputs and maximum glacial melt.

5.4.2 Drought scenario and 2002 glacier coverage

For the drought scenario simulations, I created a five-year input file using the same year of hypothetical drought conditions five years in a row (see section 4.6.2) to examine how drought affects the glacial component of streamflow in general, and to examine compounding effects of several years of drought. Following is a discussion of the results of the drought simulations.

Glacial meltwater contributions to streamflow

Simulated stream discharge ranged from $3.64 \times 10^8 \text{ m}^3$ during the first year of drought to $3.51 \times 10^8 \text{ m}^3$ during the fifth year of drought (Table 10). The higher discharge during the first year can be explained by the fact that the initial conditions for the 5-year drought simulation were defined as the end of WY 2005 (Appendix B). Therefore, more water was stored in the soil at the beginning of the simulation than at the end of any drought year simulation, resulting in a higher discharge for the first year. Glacial meltwater contribution increased slightly from 2.91% during the first year to 3.20% during the fifth year of the drought simulation (Table 10). Late-summer contribution increased from 21.4% for the first year to 32.0% during the fifth year of the drought simulation (Table 10). The most probable

explanation for this is that water which was stored in the soil decreased for each year of drought, resulting in less overall input to the stream via groundwater and an increase in the glacial meltwater component of streamflow.

Change in glacier discharge compared to present conditions

Using meteorological data for WYs 2003-2005 (the same used for model calibration and validation) and 2002 glacier coverage, simulated cumulative glacier discharge ranged from $6.95 \times 10^6 \text{ m}^3$ to $1.15 \times 10^7 \text{ m}^3$ (Table 8). After calculating the cumulative glacier discharge for the drought scenario, I compared the resulting discharge to that for present climate conditions (WYs 2003-2005). 2002 glacier coverage was used for all simulations. Following is a discussion of the results of the drought condition simulations.

The drought scenario corresponds to a change in glacier discharge between -4.3% and +59.7% compared to present climate conditions (Table 11). For these comparisons, the first year of drought was compared to WY 2003, the second year of drought was compared to WY 2004, and the third year of drought was compared to WY 2005. It makes sense that glacier discharge is generally increased for the drought scenario compared to present climate conditions because less snow is produced during a drought, and the snowpack therefore melts off earlier promoting earlier melting of the glacier and increased glacier discharge.

Decrease in stream discharge compared to present conditions

As previously mentioned, the City of Bellingham diverts water from the Middle Fork and it is therefore important to consider how a drought scenario would affect overall streamflow, and not only glacier discharge. I compared streamflow from drought

simulations to streamflow based on present climate conditions (WYs 2003-2005). 2002 glacier coverage was used for all simulations. Following is a discussion of the results of the drought simulations.

Drought conditions correspond to a decrease in annual stream discharge between 12.8% and 35.5% compared to present climate conditions (WY 2003-2005; Table 12). The decrease in late-summer stream discharge for drought simulations varies from 9.6% to 67.6% compared to present climate conditions (Table 12). This range in values is a function of comparing fairly consistent simulated data to streamflow data simulated for three different water years. For example, the streamflow for the first year of drought is compared to streamflow for WY 2003, streamflow for the second year of drought is compared to streamflow for WY 2004, and streamflow for the third year of drought is compared to streamflow for WY 2005.

The maximum decrease in summer and late-summer stream discharge consistently occurs with the water year 2004 meteorological input file for all glacier scenarios. Again, WY 2004 had the most precipitation of the three years used for meteorological input (Table 1). It makes physical sense that the largest difference in streamflow results from comparing a drought simulation to the wettest water year. The maximum decrease in stream discharge generally occurs during late-summer (Table 12). The decrease in late-summer streamflow is primarily a function of decreased precipitation and therefore less overall input to the stream, and not a function decreased glacier discharge.

5.4.3 Increased precipitation scenario and 2002 glacier coverage

As with the drought simulations, I used a one-year meteorological input file representing increased precipitation five years in a row (see section 4.6.2) to evaluate the effect of increased precipitation on the glacial component of streamflow, and to examine compounding effects of several consecutive years of increased precipitation. I then compared streamflow for the increased precipitation scenario to streamflow for present climate conditions (WYs 2003-2005). 2002 glacier coverage was used for all simulations. Following is a discussion of the results of the increased precipitation simulations.

Glacial meltwater contributions to streamflow

For the 5-year increased precipitation scenario, cumulative simulated stream discharge ranged from $6.52 \times 10^8 \text{ m}^3$ for the first year, and reached a plateau at $6.43 \times 10^8 \text{ m}^3$ for the following four years (Table 13). The glacial meltwater component of streamflow was 0.8% for all five years, while the late-summer component was 4.3% for all five years. There was no evident variability or compounding effect of multiple years of increased precipitation on glacier meltwater contribution to streamflow. The glaciers consistently began melting on June 15th or 16th, and stopped melting on October 18th.

Change in glacier discharge compared to present conditions

As with the drought simulations, I compared glacier discharge simulated for the increased precipitation scenario to that for present climate conditions (WYs 2003-2005). 2002 glacier coverage was used for all simulations. Following is a discussion of the results of the increased precipitation simulations.

The increased precipitation scenario corresponds to a decrease in glacier discharge between -27.3% and -56.0% compared to present climate conditions (Table 14). Again, for these comparisons, the first year of increased precipitation was compared to WY 2003, the second year of increased precipitation was compared to WY 2004, and the third year of increased precipitation was compared to WY 2005. It is reasonable for glacier discharge to decrease for the increased precipitation scenario compared to present climate conditions because more snow is produced during this scenario; the snowpack takes longer to melt off, and therefore results in a shorter glacier melt period and decreased glacier discharge (Table 13 and 14).

Increase in stream discharge compared to present conditions

Simulated stream discharge was consistently higher for the increased precipitation scenario than that simulated for present climate conditions (WYs 2003-2005; Table 15). Because stream discharge was the same for four of the five years simulated, I compared the simulated streamflow to that simulated for each year of present climate conditions (WYs 2003-2005). Late-summer stream discharge increased by 195.2% compared to WY 2003, by 7.8% compared to WY 2004, and by 106.7% compared to WY 2005 (Table 15). This is reasonable because WY 2004 was the wettest of the three years of present climate, while 2003 was the driest (Table 1). It is expected that the effect of increased precipitation would be reduced when compared to a wet year and amplified when compared to a dry year.

5.4.4 Predicted climate scenario with 2002 and predicted 2050 glacier coverages

The meteorological input file that was created for the predicted climate simulations was based on modeled climate change for the Pacific Northwest for the 2040s and 2050s (Climate Impacts Group, 2004). Because climate data were modified to simulate future climate, I applied DHSVM to examine the glacial meltwater contributions based on present glacier conditions (2002 coverage) and predicted glacier coverage for the same time period (17% reduction; year 2050). I compared total streamflow and the glacial meltwater component of streamflow to that simulated using present climate conditions (WYs 2003-2005) and like glacier coverages. Following is a discussion of the results of each of these simulations.

Glacial meltwater contributions to streamflow

For the 5-year predicted climate scenario and 2002 glacier coverage, cumulative simulated stream discharge ranged from $4.4 \times 10^8 \text{ m}^3$ to $5.7 \times 10^8 \text{ m}^3$ (Table 16). The glacial meltwater component of streamflow ranged from 2.2% to 3.3%. The *late-summer* meltwater component was consistently higher and ranged from 11.3% to 33.7% (Table 16). As expected, DHSVM consistently simulated lower overall streamflow and glacial meltwater contribution for the smaller glacier coverage.

Glaciers began melting earlier in the year for the predicted climate scenario, and continue melting later into the year than under present climate conditions. One explanation for this observation is that increased summer temperatures promoted the longer melting season.

Change in glacier discharge compared to present conditions

To evaluate the effect of predicted climate change on glacial melt, I compared glacier discharge simulated for the predicted climate scenario to that for present climate conditions (WYs 2003-2005). I simulated glacial melt using 2002 and 2050 (17% reduction) glacier coverages. Following is a discussion of the results of the predicted climate simulations.

The predicted climate scenario corresponds to an increase in glacier discharge between 33.9 and 60.4% for 2002 glacier coverage, and between 52.8 and 69.3% for 2050 glacier coverage; all simulations were compared to present climate conditions (Table 17). It makes sense that glacier discharge increases for the predicted climate scenario compared to present climate conditions because although winter precipitation is greater, higher summer temperatures and decreased summer precipitation promote earlier melting of the glacier, similar to that for the drought simulations. The longer glacier melt period (Table 16) and increased temperatures (Table 1) result in increased glacier discharge.

Change in stream discharge compared to present conditions

Annual stream discharge was higher for the predicted climate scenario than for present climate conditions for all simulations (Table 18). However, summer and late-summer streamflow is lower for the predicted climate scenario than for present climate conditions. As mentioned previously, it has been predicted that temperatures will increase by 1.4°C (Oct-Mar) and 1.8°C (Apr-Sep) and precipitation will increase by 5% (Oct-Mar) and decrease by 4% (Apr-Sep) (Climate Impacts Group, 2004). Resulting simulated data agree; more precipitation falls in the form of rain, there is more precipitation overall, but less

during the summer. Therefore, it makes sense that overall stream discharge increases while summer and late-summer streamflow decrease. In addition, because precipitation was multiplied by a percentage to create the predicted climate file, each meteorological data set responds differently. For example, precipitation for the wettest year, WY 2004, will be even more exaggerated by the increase in precipitation of 4% than WY 2003, in which the increase in precipitation is dampened.

5.4.5 Summary of glacial melt experiments

Present (WY 2003-2005 and 2002 glacier coverage) late summer glacial meltwater contribution to streamflow in the Middle Fork Nooksack River is estimated between 8.4% and 26.1% (Table 7). The glacial meltwater component of streamflow as a percentage depends on the total streamflow in a given year. For example, a glacier contributes a higher percentage to streamflow during a dry year when overall stream input is lower. During a wet year, when the watershed is more snow-dominated or simply has more overall water input, the effect of the glacier is reduced. Larger glaciers consistently contributed more to streamflow than smaller glaciers (Table 7). The larger glaciers began melting earlier in the year and stopped melting later in the year; the smaller glaciers had a shorter melting season than the larger glaciers.

Glacier meltwater contribution to streamflow for the drought simulations was consistently higher than that for present (“average”) climate conditions and increased throughout the five year drought period for annual and sub-annual calculations. The glaciers consistently began melting earlier in the year and stopped melting later in the year than

under present climate conditions. Under the drought conditions, streamflow in the Middle Fork was simulated to decrease by approximately 9.6% to 67.6% during late-summer.

Glacier meltwater contribution for the increased precipitation simulations was consistently lower than that for present climate conditions. Meltwater contribution to streamflow was highest for the first year of increased precipitation and then reached a plateau for remainder of the simulation period. The glacier 'melt period' was similar to that for present climate conditions for all five years of the increased precipitation simulations. Under the increased precipitation conditions, streamflow in the Middle Fork was simulated to increase by approximately 18% to 56% for annual simulations and by approximately 8% to 195% during late-summer. Again, because the original meteorological input data were multiplied by a percentage to simulate increased precipitation, each year of meteorological data behaved quite differently.

The glacier meltwater component of streamflow for the predicted climate simulations ranged from 11.3% to 33.7% during late-summer with 2002 glacier coverage. Glacier contribution was generally higher for this scenario than for present climate conditions (WYs 2003-2005). Under the predicted climate conditions, streamflow in the Middle Fork was simulated to increase by approximately 3% to 5% for annual simulations and decrease by approximately 6% to 10% during late-summer. The overall increase in stream discharge is the result of increased (and warmer) winter precipitation, while the decrease in summer stream discharge is the result of decreased summer precipitation. The glaciers began melting earlier in the year and stopped melting later in the year than under present climate conditions as a result of increased precipitation in the form of rain and increased summer temperatures.

5.5 Implications

A decrease in the glacial meltwater component of streamflow, especially during late-summer, could have substantial implications for water resources in Whatcom County, WA. Water use is highest during late-summer when streamflow is lowest. The city could potentially store excess water during the winter months to compensate for water shortages during the summer when demand is highest. However, the city presently maintains the maximum storage capacity in Lake Whatcom in the spring, so any increased storage would require other storage facilities.

Ecological issues such as salmon habitat and migration as well as flooding issues continue to govern Middle Fork water resources management. These issues will likely become more problematic in the future, especially during late-summer, as a result of both climate change and glacier shrinkage. The viability of the Middle Fork Nooksack diversion in the late summer may be compromised as a result of low stream discharge during that time.

6.0 CONCLUSIONS

The major goals of this thesis were to quantify present glacial meltwater contribution to streamflow in the Middle Fork Nooksack River, and to examine the relationship between glacier size and runoff under a variety of climate conditions at annual and sub-annual time scales. I accomplished this objective with the use of the Distributed Hydrology Soils Vegetation Model (DHSVM). DHSVM simulates a water and energy balance at the pixel scale of a DEM. All hydrologic parameters in the basin, including soil type and thickness, vegetation classifications, and glacier coverage are defined at the pixel scale. Applying the

model using a variety of glacier sizes along with variable climate conditions has provided the first detailed, quantitative information on the timing and contribution of snow and glacier melt in the Middle Fork basin.

DHSVM simulations were performed at a 1-hour time-step for WYs 2003-2005, and with hypothetical meteorological input files. GIS pixel resolution was set at 50 m x 50 m for all simulations. SWE was well represented by DHSVM when compared to that measured at the Middle Fork SNOTEL site. Stream discharge and timing were also well represented when compared to that recorded at the USGS stream gauge. Peak stream discharge was typically underestimated by DHSVM; however, the quality of discharge measurements above 4,000 cfs is considered poor by the USGS. Summer streamflow was slightly underestimated and is likely due to poor constraints on the amount and distribution of snow in the basin.

The calibrated model was used to simulate streamflow under present climate conditions and hypothetical climate conditions including drought, increased precipitation, and predicted climate conditions. It was also applied using a variety of glacier coverages including the estimated LIA maximum extent, 2002 coverage, 17% reduction in glacier size (predicted for year 2050), and 48% reduction in glacier size (predicted for year 2150). Applying DHSVM in this manner, I was able to establish a non-linear relationship between glacier size and meltwater contribution to streamflow based on present climate conditions (Figure 29). Based on combinations of the above variable climate conditions and glacier coverages, the major conclusions of this study are as follows.

Glacial meltwater component of late-summer streamflow

1. The glacial meltwater component of late-summer streamflow as defined by the 2002 glacier coverage and *present climate conditions* ranged from 8.4% to 26.1%.
2. The glacial meltwater component of late-summer streamflow as defined by the 2002 glacier coverage and *drought conditions* ranged from 21.4% to 32.0%.
3. The glacial meltwater component of late-summer streamflow as defined by the 2002 glacier coverage and *increased precipitation* conditions was steady at 4.3%.
4. The glacial meltwater component of late-summer streamflow as defined by the 2002 glacier coverage and *predicted climate conditions* ranged from 11.3% to 33.7%.

Decrease in late-summer streamflow as a result of glacier shrinkage

1. A 17% reduction in glacier size (predicted for year 2050) may result in a decrease in late-summer stream discharge of 3.1% to 8.6% with present climate conditions.
2. A 48% reduction in glacier size (predicted for year 2150) may result in a decrease in late-summer stream discharge of 6.7% to 19.4% with present climate conditions.

Increase/decrease in late-summer streamflow as a result of variable climate scenarios

1. Drought conditions may result in a *decrease* in late-summer stream discharge of 9.6% to 67.6%.
2. Increased precipitation conditions may result in an *increase* in late-summer stream discharge of 7.8% to 195.2%.
3. Predicted climate conditions may result in a *decrease* in late-summer stream discharge of 6.2% to 10.2% with the 2002 glacier coverage.
4. Predicted climate conditions may result in a *decrease* in late-summer stream discharge of 8.7% to 15.7% with the predicted 2050 glacier coverage.

Timing and volume of glacial melt

1. The glacial melt period typically lasts from mid-June through mid-October for glaciers defined at their 2002 extent and under present climate conditions. Glaciers begin melting slightly earlier, stop melting slightly later, and produce more discharge during a dry year than a wet year.
2. The timing of glacial melt is similar for present conditions and the increased precipitation scenario. Glaciers began melting earlier in the year and stopped melting later in the year for the drought and predicted climate scenarios.

7.0 FUTURE WORK

Deming glacier meltwater is an essential component of the water resources for the City of Bellingham, WA. Future monitoring of the glacial component of streamflow, not only in the Middle Fork but in the greater Nooksack River, is crucial to assess future water resource management in Whatcom County. I provide the following recommendations to improve this application of DHSVM and to evaluate the effects of glaciers throughout the Nooksack watershed.

- Incorporate the use of PRISM precipitation grids into this application of DHSVM.
- Incorporate the use of multiple stations into this application of DHSVM.
- Evaluate the effect of deglaciation on the Nooksack watershed. The South Fork of the Nooksack is not glaciated, but the North Fork is. Create a DHSVM model of the North Fork and apply DHSVM to examine the effect and implications of deglaciation on the entire Nooksack watershed.
- Examine more rigorously the influence of climate change and drought conditions.

8.0 REFERENCES

- Arnold, N. S., I. C. Willis, M.J. Sharp, K. S. Richards, and W. J. Lawson, 1996, A distributed surface energy-balance model for a small valley glacier. I. Development and testing for Haut Glacier d'Arolla, Valais, Switzerland, *Journal of Glaciology*, v. 42, n. 42, p. 77-88.
- Bach, A. J., 2002, Snowshed contributions to the Nooksack River watershed, North Cascades Range, Washington, *Geographical Review* 92: 192-212.
- Benn, D. I. and D. J. A. Evans, 1998, *Glaciers and Glaciation*, First Edition, Arnold. London.
- Bowling, L. and D. P. Lettenmaier, 2001, The effects of forest roads and harvest on catchment hydrology in a mountainous maritime environment. *American Geophysical Union, Water Science and Application Volume 2*, p. 145-164.
- Chennault, J., 2004, Modeling the contributions of glacial meltwater to streamflow in Thunder Creek, North Cascades National Park, Washington. Western Washington University Master's Thesis.
- Clark, Doug, 2006-2007, Personal Communications. Professor of Geology, Western Washington University, Bellingham, Washington.
- Climate Impacts Group, 2004, Climate change scenarios for the Pacific Northwest <http://cses.washington.edu/cig/fpt/ccscenarios.shtml>
- Dingman, S. L., 2002, *Physical Hydrology*, Prentice hall, 646 p.
- Ecology (Washington State Department), 1985, Nooksack Instream Resources Protection Program, W.W.I.R.P.P. Series no. 11, Chapter 173-501 WAC, <http://www.ecy.wa.gov/pubs/93020.pdf>.
- Fountain, A. G. and W. V. Tangborn, 1985, The effect of glaciers on streamflow variations, *Water Resources Research* 21(4): 579-586.
- Fountain, A. G., R. M. Krimmel and D. C. Trabant, 1997, A Strategy for monitoring glaciers, *USGS Circular* 1132, 19 pp.
- Franklin, J. F. and C. T. Dyrness, 1973, *Natural vegetation of Oregon and Washington*, U.S. Forest Service: 452.
- Fuller, S. R., 1980, Neoglaciation of Avalanche Gorge and the Middle Fork Nooksack River Valley, Mt. Baker, Washington. Western Washington University Master's Thesis.

- Gardner, C. A., K. M. Scott, C. D. Miller, B. Myers, W. Hildreth, P. T. Pringle, 1995, Potential volcanic hazards from future activity of Mount Baker, Washington, USGS.
- Goldin, A. 1992, Soil survey of Whatcom County area, Washington, United States Department of Agriculture, Soil conservation service.
- Granshaw F. D., 2002, Glacier change in the North Cascades National Park Complex, Washington State, USA, 1958-1998. University of Portland Master's Thesis.
- Greenberg, Joanne, P.E., 2007, Personal Communications. Water Resources Engineer, HydroLogic Services Co., Bellingham, WA.
- Harper, J. T., 1992, The dynamic response of glacier termini to climatic variation during the period 1940-1990 on Mount Baker, Washington, U.S.A. Western Washington University Master's Thesis.
- Kelleher, K., 2006, Streamflow calibration of two sub-basins in the Lake Whatcom Watershed, Washington using a distributed hydrology model. Western Washington University Master's Thesis.
- Krimmel, R. M., 1992, Runoff from two mountain basins in the North Cascades, Washington, U.S.A., AGU 1992 Fall Meeting, EOS, Transaction, American Geophysical Union 73(43): 180.
- Martinec, J. and A. Rango, 1986, Parameter values for snowmelt runoff modeling, Journal of Hydrology 84(3-4): 197-219.
- Meier, M. F. 1984, Contributions of small glaciers to global sea level, Science 226: 1418-1421.
- Meier, M. F., 1986, Snow, ice and climate; their contribution to water supply, USGS Water-Supply Paper: 69-82.
- Miller D. A. and R. A. White, 1998, A conterminous United States multi-layer soil characteristics data set for regional climate and hydrology modeling, Earth Interactions, col. 2, (<http://EarthInteractions.org>).
- Pelto, M. S., 1991, Glacier runoff into Baker Lake, Washington, AGU-MSA 1991 Spring Meeting, EOS, Transaction, American Geophysical Union 72(17): 130.
- Pelto, M. S. 1996, Annual net balance of North Cascade Glaciers 1984-1994, Journal of Glaciology, v. 41, p. 3-9.
- Pelto, M. S. and J. Riedel, 2001, Spatial and temporal variations in annual balance of North Cascades Glaciers, Washington U.S.A., Journal of Glaciology, v. 47, p 497-506.

Pelto, M. S., 2003, Contribution of the Deming Glacier to streamflow in the Middle Fork Nooksack River 2002 and 2003 summer melt seasons, <http://www.nichols.edu/departments/glacier/deming.pdf>

Post, A., D. Richardson, W. V. Tangborn, F. L. and Rosselot, 1971, Inventory of glaciers in North Cascades, Washington, USGS.

Rango, A., J. F. Hannaford, R. L. Hall, M. Rosenzweig, and A. J. Brown, 1979, Snow covered area utilization in runoff forecasts, *Journal of the Hydraulics Division*, v. 105, n. HY 1, p. 53-66.

Rango, A., 1988, Evaluating the effects of climate change on snowmelt hydrology of mountain basins, AGU 1988 fall meeting, EOS, Transactions, American Geophysical Union, v. 69, n. 44, p. 1203

Riedel, J. L., A. Fountain, and B. Krimmel, 1999, Glacier Monitoring Program: North Cascades, Progress Report. (<http://www.nps.gov/noca/massbalance.htm>).

Scott, K., 2006, Personal Communications. USGS Geologist, Cascades Volcano Observatory, Washington.

Storck, P., D. P. Lettenmaier, B.A. Connelly, and T. W. Cundy, 1995, Implications of forest practices on downstream flooding: Phase II Final Report, Washington Forest Protection Association, TFW-SH20-96-001, 100 p.

Storck, P., L. Bowling, P. Wetherbee, and D. Lettenmaier, 1998, Application of a GIS-based hydrology model for prediction of forest harvest effects on peak streamflow in the Pacific Northwest, *Hydrology Processes*, v. 12, n. 6, p. 653-658.

Tangborn, W.V., R. M. Krimmel, and M. F. Meier, 1975, A comparison of glacier mass balance by glaciological, hydrological and mapping methods, *South Cascade Glacier*, Washington, IAHS-AISH Publication, n. 104, p. 185-196.

Tangborn, W. V., 1980, Two models for estimating climate-glacier relationships in the North Cascades, Washington, U.S.A., *Journal of Glaciology* 25(1): 3-21.

Tracy, K., 2001. Changes in Mirror Lake, northwestern Washington as a result of the diversion of water from the Nooksack River. Western Washington University Master's Thesis.

USGS, 2005, Water resources of Washington State, <http://wa.water.usgs.gov/data/realtime/htmls/Nooksack.html>.

Vogel, 1984, Performance of catalytically condensed carbon for use in accelerator mass spectrometry, *Nuclear instruments and methods in physics research*, pp. 289-293.

Walker, S. J., 1995, A hydrologic model for the Lake Whatcom Watershed: development, implementation, and assessment. Western Washington University Master's Thesis.

Wigmosta, M. S., L. W. Vail, and D. P. Lettenmaier., 1994, A distributed hydrology-vegetation model for complex terrain, *Water Resources Research* 30(6): 1665-1679.

Wigmosta, M. S. and W. A. Perkins, 2001, Simulating the effects of forest roads on watershed hydrology, American Geophysical Union, *Water Science and Application* Volume 2, p. 127-143.

Wigmosta, M.S., B. Nijssen, P. Storck, and D. P. Lettenmaier, 2002, The Distributed Hydrology Soil Vegetation Model, In *Mathematical Models of Small Watershed Hydrology and Applications*, V.P. Singh, D.K. Frevert, eds., Water Resource Publications, Littleton, CO., p. 7-42.

TABLES

		Clearbrook Station		Middle Fork SNOTEL		Predicted Climate		Drought		Increased Precipitation	
		Precipitation sum (m)	Temperature (Average)	Precipitation sum (m)	Temperature (Average)						
WY 2003	Oct	0.28	12.2	0.06	5.95	0.06	7.35	0.06	5.30	0.59	5.30
	Nov	0.17	4.4	0.35	4.92	0.37	6.32	0.35	1.93	0.57	1.93
	Dec	0.07	4.5	0.34	0.27	0.36	1.67	0.33	0.75	0.34	0.75
	Jan	0.15	-4	0.42	2.71	0.44	4.11	0.41	0.14	0.43	0.14
	Feb	0.05	4.63	0.17	0.64	0.18	1.49	0.13	1.68	0.17	1.68
	Mar	0.13	6.93	0.52	-0.37	0.55	1.03	0.26	1.82	0.52	1.82
	Apr	0.09	9.5	0.21	1.47	0.20	3.27	0.04	3.61	0.23	3.61
	May	0.07	12.5	0.10	4.77	0.10	6.57	0.10	7.41	0.15	7.41
	Jun	0.04	16.5	0.08	9.94	0.07	11.74	0.07	6.76	0.12	6.76
	Jul	0.06	17.9	0.02	13.12	0.01	14.92	0.02	11.30	0.10	11.30
	Aug	0.01	17.3	0.01	12.59	0.01	14.39	0.01	13.17	0.19	13.17
	Sep	0.04	15.6	0.12	11.00	0.12	12.77	0.12	7.33	0.27	7.33
	SUM	1.16	NA	2.40	NA	2.47	NA	1.90	NA	3.68	NA
WY 2004	Oct	0.14	10.9	0.59	6.55	0.62	7.95	0.06	5.30	0.59	5.30
	Nov	0.19	5.9	0.57	-1.09	0.60	0.31	0.35	1.93	0.57	1.93
	Dec	0.19	4.9	0.33	-1.07	0.34	0.32	0.33	0.75	0.34	0.75
	Jan	0.15	3.1	0.41	-0.91	0.43	0.49	0.41	0.14	0.43	0.14
	Feb	0.06	6.1	0.13	0.53	0.13	1.93	0.13	1.68	0.17	1.68
	Mar	0.13	8.6	0.34	1.50	0.36	2.90	0.26	1.82	0.52	1.82
	Apr	0.03	11.8	0.04	5.27	0.04	7.07	0.04	3.61	0.23	3.61
	May	0.08	13.7	0.15	5.54	0.14	7.34	0.10	7.41	0.15	7.41
	Jun	0.03	16.8	0.08	10.84	0.08	12.64	0.07	6.76	0.12	6.76
	Jul	0.02	19.1	0.02	3.47	0.02	15.27	0.02	11.30	0.10	11.30
	Aug	0.10	19.1	0.19	13.67	0.19	15.47	0.01	13.17	0.19	13.17
	Sep	0.13	14.5	0.27	7.55	0.26	9.35	0.12	7.33	0.27	7.33
	SUM	1.23	NA	3.12	NA	3.21	NA	1.90	NA	3.68	NA
WY 2005	Oct	0.18	11.3	0.25	5.30	0.26	6.70	0.06	5.30	0.59	5.30
	Nov	0.12	5.2	0.47	1.93	0.49	3.33	0.35	1.93	0.57	1.93
	Dec	0.14	4.0	0.34	0.75	0.36	2.15	0.33	0.75	0.34	0.75
	Jan	0.20	3.2	0.43	0.14	0.45	1.54	0.41	0.14	0.43	0.14
	Feb	0.05	5.2	0.13	1.68	0.13	3.08	0.13	1.68	0.17	1.68
	Mar	0.15	8.4	0.26	1.82	0.27	3.22	0.26	1.82	0.52	1.82
	Apr	0.12	9.9	0.23	3.61	0.22	5.41	0.04	3.61	0.23	3.61
	May	0.09	14.7	0.13	7.41	0.13	9.21	0.10	7.41	0.15	7.41
	Jun	0.05	15.6	0.12	6.76	0.12	8.56	0.07	6.76	0.12	6.76
	Jul	0.03	17.8	0.10	11.30	0.10	13.10	0.02	11.30	0.10	11.30
	Aug	0.04	18.0	0.04	13.17	0.04	14.97	0.01	13.17	0.19	13.17
	Sep	0.08	14.1	0.21	7.33	0.20	9.13	0.12	7.33	0.27	7.33
	SUM	1.26	NA	2.71	NA	2.77	NA	1.90	NA	3.68	NA
75 year average	Oct	0.11	10.3								
	Nov	0.16	5.9								
	Dec	0.15	3.1								
	Jan	0.13	2.9								
	Feb	0.11	4.9								
	Mar	0.1	7.2								
	Apr	0.09	9.9								
	May	0.08	13								
	Jun	0.07	15.3								
	Jul	0.05	17.4								
	Aug	0.04	17.4								
	Sep	0.07	14.8								
	SUM	1.16	NA								

Table 1: Monthly precipitation sums and monthly average temperature for meteorological data used as model input.

Vegetation Parameter	Vegetation Type								
	4	5	8	10	12	13	14	15	20
	Deciduous Broadleaf	Mixed Forest	Closed Shrub	Grassland	Bare	Urban	Water	Coastal Conifer	Glacier
Impervious fraction	0.0	0.0	0.0	0.0	0.0	0.0	0.0	0.0	0.0
Max Snow Int Capacity	0.003	0.003	NA	NA	NA	NA	NA	0.04	NA
Vapor pressure deficit	4.0E+03	4.0E+03	4.0E+03	4.0E+03	NA	4.0E+03	NA	4.0E+03	NA
# of root zones	3	3	3	3	3	3	3	3	3
Overstory LIA	Variable 2.0-10.0	Variable 2.0-6.0	Variable 1.0-4.0	Variable 0.5-6.0	0.0	Variable 1.0-3.0	0.0	12.0	0.0
Understory LIA	Variable 2.0-3.0	Variable 2.0-3.0	Variable 1.0-4.0	0.19	0.0	Variable 1.0-3.0	0.0	3.0	0.0
% of Middle Fork basin	1.4%	3.1%	19.0%	2.2%	5.8%	0.1%	0.1%	65.1%	3.1%

Table 2: Vegetation hydrologic parameters For Middle Fork basin. For a complete list of vegetation hydrologic parameters refer to the DHSVM webpage: www.hydro.washington.edu/Lettenmaier/Models/DHSVM/index.htm

63

Soil Parameter	Soil Type						
	1	3	5	6	8	14	15
	Sand	Sandy Loam	Silt	Loam	Silty Clay Loam	Water (as clay)	Bedrock
Lateral conductivity	0.01	0.01	0.01	0.02	0.01	0.01	0.01
Vertical conductivity	0.01	0.01	0.01	0.01	0.01	0.01	0.01
Maximum infiltration	2.00E-04	3.00E-05	3.00E-05	1.00E-05	3.00E-05	1.00E-05	1.00E-05
Porosity	0.43	0.4	0.52	0.43	0.48	0.47	0.1
Filed Capacity	0.08	0.21	0.28	0.29	0.36	0.36	0.05
Bulk Density	1492	1569	1280	1485	1381	1394	1650
% of Middle Fork basin	3.7%	8.4%	2.1%	14.5%	50.7%	13.0%	7.5%

Table 3: Soil hydrologic parameters for Middle Fork basin. For a complete list of soil hydrologic parameters refer to the DHSVM webpage: www.hydro.washington.edu/Lettenmaier/Models/DHSVM/index.htm

Station	UTM Coordinates		Altitude (m AMSL)
	East	North	
Wells Creek SNOTEL	589486	5412391	1280
Elbow Lake SNOTEL	580957	5393360	975
Middle Fork SNOTEL	579280	5407790	1518
North Shore weather station	548924	5399557	126
USGS stream gauge	565385	5403163	177

Table 4: Location of weather and stream gauging stations used for this thesis. Coordinates are UTM Zone 10, datum NAD 27.

Time Period	Glacier coverage in MF basin		
	% change from 2002 glacier size	Km ²	% of basin
LIA (estimated)	+144%	19.8	7.6
2002 (From NOAA)	0%	8.1	3.1
2050 (predicted)	-17%	6.7	2.6
2150 (predicted)	-48%	4.2	1.6

Table 5: Glacier coverage in the Middle Fork basin for discrete time periods.

	Snow-water equivalent	
	Simulated (m)	Measured (m)
Oct	0.01	0.01
Nov	0.07	0.07
Dec	0.19	0.21
Jan	0.25	0.25
Feb	0.29	0.25
Mar	0.29	0.31
Apr	0.46	0.67
May	0.27	0.34
Jun	0.17	0.00
Jul	0.08	0.00
Aug	0.04	0.00
Sep	0.02	0.00
SUM	2.12	2.12

Table 6: Measured and simulated monthly average snow-water equivalent defined at the Middle Fork SNOTEL station.

Present Climate Conditions (WY 2003-2005)							
Glacier Coverage	Meteorological Input file	Total Simulated discharge (m ³)	% Annual (Oct-Sep)	% Summer (Jun-Sep)	% Late-summer (Aug-Sep)	Start melt	End melt
144% increase (LIA)	WY 2003	4.57E+08	10.8	38.6	56.8	May 06	Nov 7
	WY 2004	5.87E+08	9.2	24.2	27.5	Apr 30	Oct 23
	WY 2005	5.08E+08	7.6	24.9	35.2	Apr 24	NA*
2002	WY 2003	4.18E+08	2.3	12.3	26.1	Jun 14	Oct 14
	WY 2004	5.45E+08	2.1	6.6	8.4	Jun 15	Oct 20
	WY 2005	4.76E+08	1.5	5.8	11.1	Jun 15	NA*
17% decrease (2050)	WY 2003	4.13E+08	1.3	7.8	19.2	Jun 28	Oct 13
	WY 2004	5.40E+08	1.3	4.0	5.5	Jun 23	Oct 20
	WY 2005	4.73E+08	0.8	3.2	6.9	Jun 28	NA*
48% decrease (2150)	WY 2003	4.09E+08	0.2	2.6	8.3	Jul 06	Oct 8
	WY 2004	5.36E+08	0.4	1.2	1.8	Jul 01	Oct 06
	WY 2005	4.70E+08	0.2	0.8	2.0	Jul 23	NA*

Table 7: Contribution of glacial meltwater to streamflow in the Middle Fork Nooksack River produced by present meteorological conditions (WY 2003-2005) and different glacier sizes.

*The glaciers were still melting at the end of the three-year model simulation.

Present Climate Conditions (WY 2003-2005)			
Glacier Coverage	Meteorological Input file	Simulated glacier discharge (accumulated; m³)	% Change (Jun-Sep)
144% increase (LIA)	WY 2003	4.92E+07	347.1
	WY 2004	5.40E+07	354.6
	WY 2005	3.87E+07	435.3
2002	WY 2003	9.67E+06	0.0
	WY 2004	1.15E+07	0.0
	WY 2005	6.95E+06	0.0
17% decrease (2050)	WY 2003	5.27E+06	-39.7
	WY 2004	6.86E+06	-40.2
	WY 2005	3.75E+06	-45.9
48% decrease (2150)	WY 2003	9.95E+05	-81.3
	WY 2004	2.00E+06	-82.7
	WY 2005	8.62E+05	-87.3

Table 8: Change in glacial meltwater discharge produced by present meteorological conditions and different glacier coverages (all compared to 2002 glacier coverage).

Present Climate Conditions (WY 2003-2005)					
Glacier Coverage	Meteorological Input file	Total Simulated discharge (m³)	% Annual (Oct-Sep)	% Summer (Jun-Sep)	% Late-summer (Aug-Sep)
144% increase (LIA)	WY 2003	4.57E+08	9.46	42.7	70.95
	WY 2004	5.87E+08	7.75	23.3	26.39
	WY 2005	5.08E+08	6.67	25.34	37.2
2002	WY 2003	4.18E+08	0.0	0.0	0.0
	WY 2004	5.45E+08	0.0	0.0	0.0
	WY 2005	4.76E+08	0.0	0.0	0.0
17% decrease (2050)	WY 2003	4.13E+08	-1.05	-4.88	-8.63
	WY 2004	5.40E+08	-0.85	-2.64	-3.05
	WY 2005	4.73E+08	-0.67	-2.67	-4.46
48% decrease (2150)	WY 2003	4.09E+08	-2.07	-10.01	-19.43
	WY 2004	5.36E+08	-1.74	-5.43	-6.7
	WY 2005	4.70E+08	-1.28	-5.09	-9.31
144% increase (LIA)	WY 2003	4.08E+08	-2.31	-12.3	-26.14
	WY 2004	5.33E+08	-2.16	-6.57	-8.4
	WY 2005	4.69E+08	-1.46	-5.82	-11.1

Table 9: Change in total stream discharge produced by present meteorological conditions and different glacier coverages (all compared to 2002glacier coverage).

Synthetic 5-year Drought							
Glacier Coverage	Synthetic Year	Total Simulated discharge (m ³)	% Annual (Oct-Sep)	% Summer (Jun-Sep)	% Late-summer (Aug-Sep)	Start melt	End melt
2002	1 yr	3.64E+08	2.91	14.2	21.4	May 09	Oct 30
	2 yr	3.51E+08	3.15	14.6	22.5	May 09	Oct 30
	3 yr	3.52E+08	3.15	14.6	31.5	May 13	Oct 31
	4 yr	3.51E+08	3.2	14.8	31.9	May 09	Oct 30
	5 yr	3.51E+08	3.2	14.8	32.0	May 09	NA

Table 10: Contribution of glacial meltwater to streamflow in the Middle Fork Nooksack River based a hypothetical drought s cenario. The drought file was used to simulate streamflow for 2002 glacier coverage.

Synthetic 5-year Drought			
Glacier Coverage	Synthetic Year	Simulated glacier discharge (m ³)	% Change (Jun-Sep)
2002	1 yr	1.06E+07	9.6
	2 yr	1.10E+07	-4.3
	3 yr	1.11E+07	59.7

Table 11: Change in glacial meltwater produced by drought conditions and 3.1% glacier coverage (compared to meteorological conditions for WYs 2003-2005 and 2002 glacier coverage).

Synthetic Drought for year 2050 (WY 2003-2005)						
Glacier Coverage	Synthetic Year	Simulated discharge for drought conditions (m ³)	Simulated discharge for WY 2003-2005 (m ³)	% Annual (Oct-Sep)	% Summer (Jun-Sep)	% Late-summer (Aug-Sep)
2002	1 yr	3.64E+08	4.18E+08	-12.8	-21.6	-9.6
	2 yr	3.51E+08	5.45E+08	-35.5	-55.8	-67.6
	3 yr	3.52E+08	4.76E+08	-26	-35.7	-37.8

Table 12: Decrease in total stream discharge produced by drought conditions and 3.1% glacier coverage (compared to meteorological conditions for WYs 2003-2005 and 2002 glacier coverage)

Increased Precipitation							
Glacier Coverage	Synthetic Year	Total Simulated discharge (m ³)	% Annual (Oct-Sep)	% Summer (Jun-Sep)	% Late-summer (Aug-Sep)	Start melt	End melt
2002	1 yr	6.52E+08	0.8	2.9	4.3	Jun 15	Oct 18
	2 yr	6.43E+08	0.8	2.9	4.3	Jun 15	Oct 18
	3 yr	6.43E+08	0.8	2.9	4.3	Jun 16	Oct 18
	4 yr	6.43E+08	0.8	2.9	4.3	Jun 16	Oct 18
	5 yr	6.43E+08	0.8	2.9	4.3	Jun 16	NA

Table 13: Contribution of glacial meltwater to streamflow in the Middle Fork Nooksack River based increased precipitation scenario. The increased precipitation file was used to simulate streamflow for 2002 glacier coverage.

Increased Precipitation			
Glacier Coverage	Synthetic Year	Simulated glacier discharge (m ³)	% Change (Jun-Sep)
2002	1 yr	5.05E+06	-47.8
	2 yr	5.06E+06	-56.0
	3 yr	5.05E+06	-27.3

Table 14: Change in glacial meltwater produced by increased precipitation conditions and 2002 glacier coverage (compared to meteorological conditions for WYs 2003-2005 and 2002 glacier coverage).

Increased Precipitation						
Glacier Coverage	Synthetic Year	Simulated discharge for increased precipitation (m ³)	Simulated discharge for WY 2003-2005 (m ³)	% Annual (Oct-Sep)	% Summer (Jun-Sep)	% Late-summer (Aug-Sep)
2002	1 yr	6.52E+08	4.18E+08	56.18	83.73	195.19
	2 yr	6.43E+08	5.45E+08	18.06	5.27	7.8
	3 yr	6.42E+08	4.76E+08	35.01	49.59	106.65

Table 15: Increase in total stream discharge produced by increased precipitation conditions and 2002 glacier coverage (compared to meteorological conditions for WYs 2003-2005 and 2002 glacier coverage).

Predicted Climate for year 2050							
Glacier Coverage	Meteorological Input file	Total Simulated discharge (m ³)	% Annual (Oct-Sep)	% Summer (Jun-Sep)	% Late-summer (Aug-Sep)	Start melt	End melt
2002	Adjusted 2003	4.37E+08	3.26	21.0	33.7	Jun 01	Nov 02
	Adjusted 2004	5.66E+08	2.74	10.0	11.3	May 25	Oct 20
	Adjusted 2005	4.91E+08	2.23	10.5	16.1	May 12	NA
2050	Adjusted 2003	4.31E+08	2	14.6	26.2	June 09	Oct 31
	Adjusted 2004	5.60E+08	1.73	6.5	7.9	June 16	Oct 20
	Adjusted 2005	4.87E+08	1.31	6.4	10.9	June 10	NA

Table 16: Contribution of glacial meltwater to streamflow in the Middle Fork Nooksack River based on a predicted future climate scenario. The file was used to simulate streamflow for 2002 and predicted 2050 glacier coverages.

71

Predicted Climate for year 2050			
Glacier Coverage	Meteorological Input file	Simulated glacier discharge (m ³)	% Change (Jun-Sep)
2002	Adjusted 2003	1.43E+07	47.9
	Adjusted 2004	1.54E+07	33.9
	Adjusted 2005	1.07E+07	60.4
2050	Adjusted 2003	8.64E+06	63.9
	Adjusted 2004	9.62E+06	52.8
	Adjusted 2005	6.35E+06	69.3

Table 17: Change in glacial meltwater produced by predicted climate conditions and 2002 glacier coverage (compared to meteorological conditions for WYs 2003-2005 and 2002 glacier coverage).

Predicted Climate for year 2050						
Glacier Coverage	Meteorological Input file	Simulated discharge for predicted climate (m ³)	Simulated discharge for WY 2003-2005 (m ³)	% Annual (Oct-Sep)	% Summer (Jun-Sep)	% Late-summer (Aug-Sep)
2002	Adjusted 2003	4.37E+08	4.18E+08	4.62	-19.64	-6.23
	Adjusted 2004	5.66E+08	5.45E+08	3.77	-12.76	-5.14
	Adjusted 2005	4.91E+08	4.76E+08	3.22	-12.81	-10.2
2050	Adjusted 2003	4.31E+08	4.13E+08	3.27	-25.7	-15.74
	Adjusted 2004	5.60E+08	5.40E+08	2.71	-15.98	-8.68
	Adjusted 2005	4.87E+08	4.73E+08	2.25	-16.58	-15.44

Table 18: Change in stream discharge produced by the predicted climate scenario for 2002 and predicted 2050 glacier coverage (compared to meteorological conditions for WYs 2003-2005 and 2002 and 2050 glacier coverage, respectively).

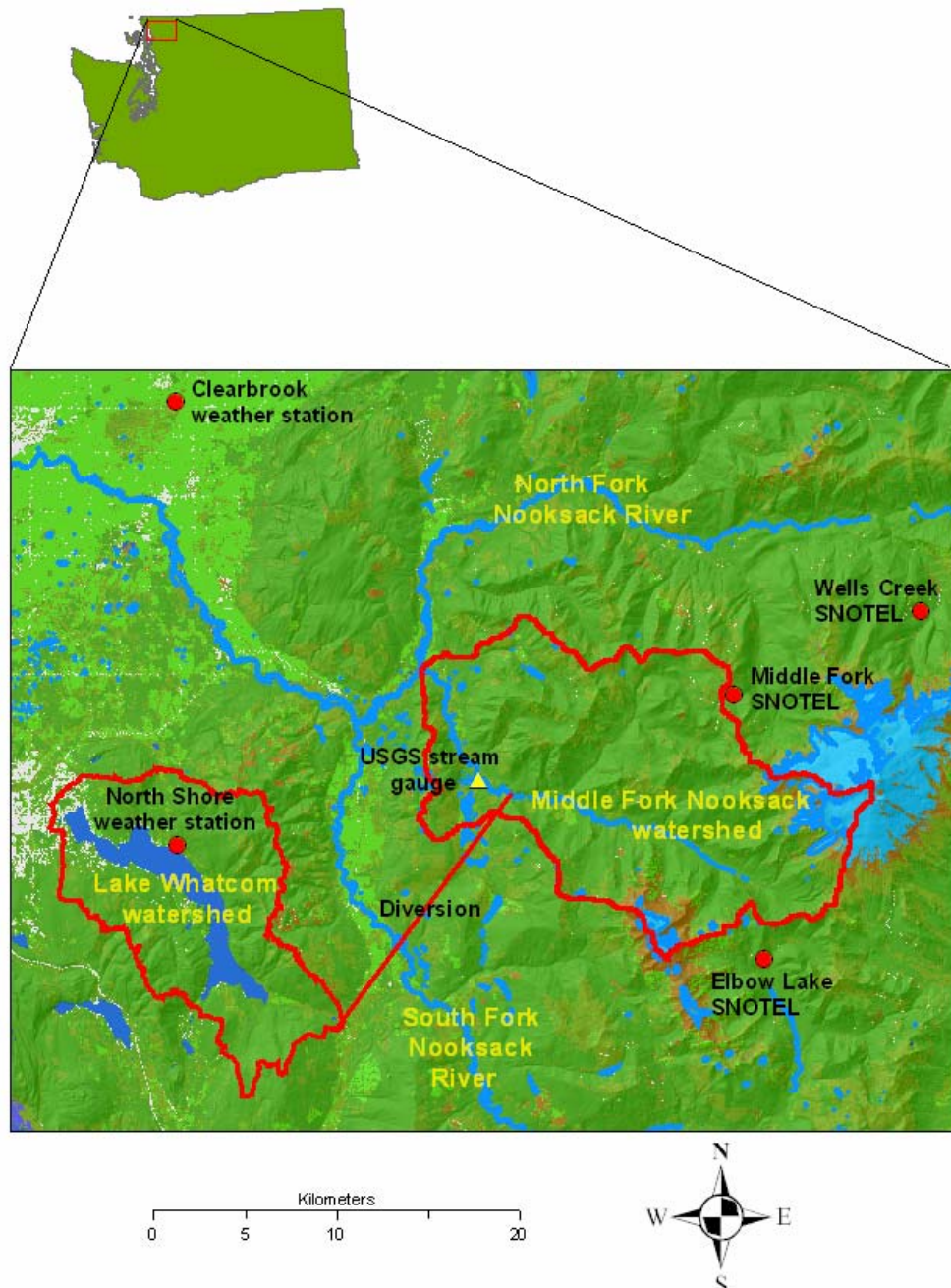


Figure 1: Location of weather stations and stream gauge, main tributaries of the Nooksack River, the Middle Fork Nooksack River watershed, Lake Whatcom watershed, and the Middle Fork diversion, western Whatcom County, Washington.

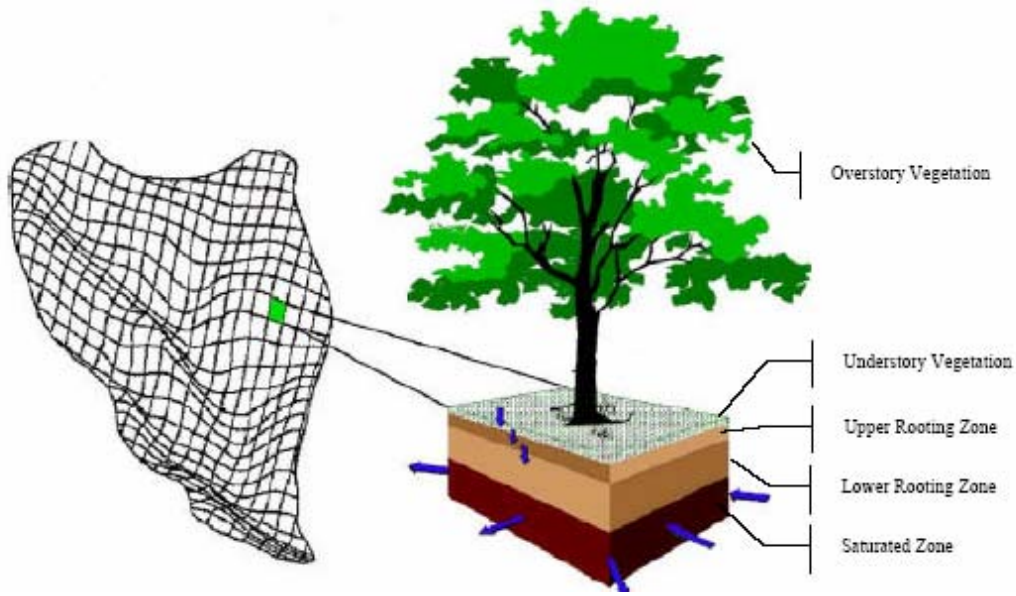


Figure 2: Schematic diagram of DHSVM structure. All modeling is based on established hydrologic relationships and each grid cell is able to exchange water with all adjacent cells (Modified from Wigmosta, 2001).

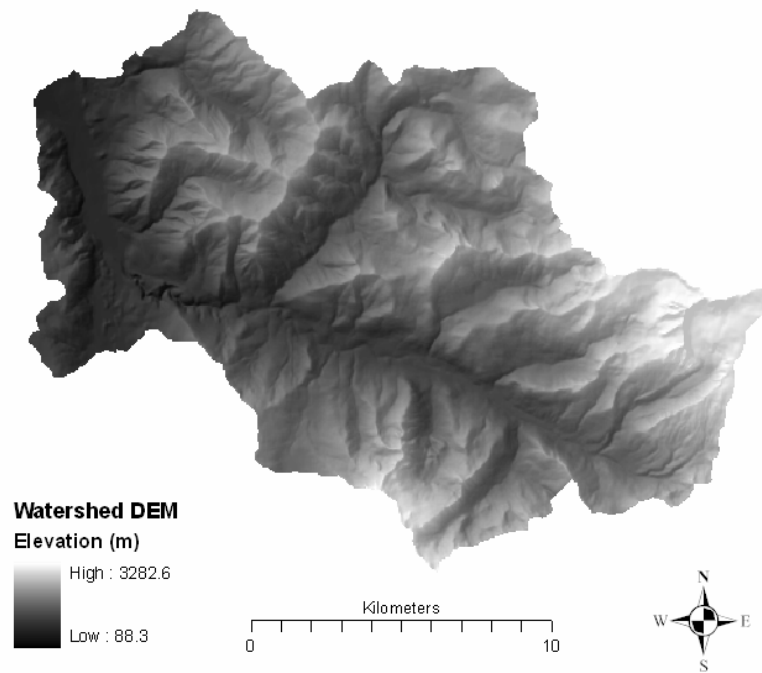


Figure 3: Digital Elevation Model (DEM) for the Middle Fork Nooksack River basin.

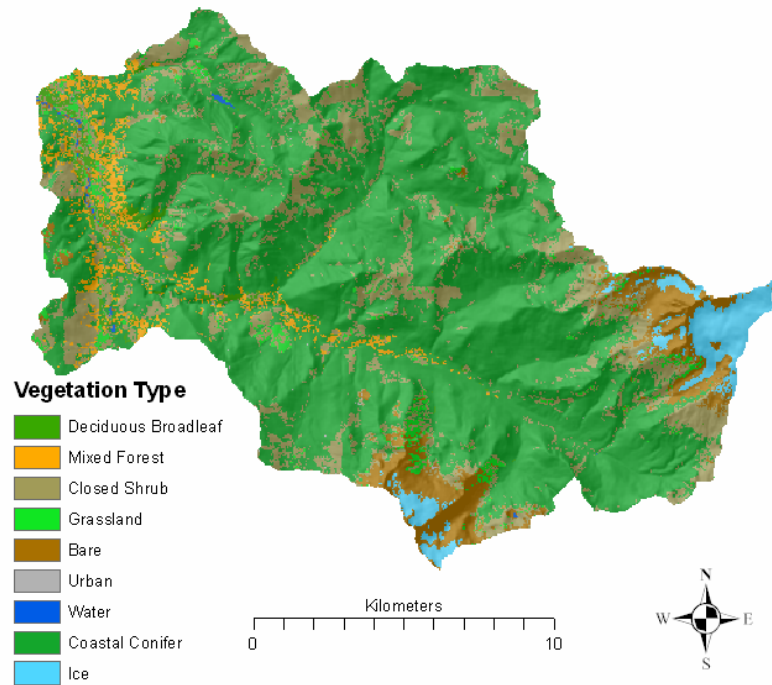


Figure 4: Vegetation classifications for the Middle Fork Nooksack River basin. Data were obtained from NOAA, 2002 (<http://www.csc.noaa.gov/crs/lca/pacificcoast.html>).

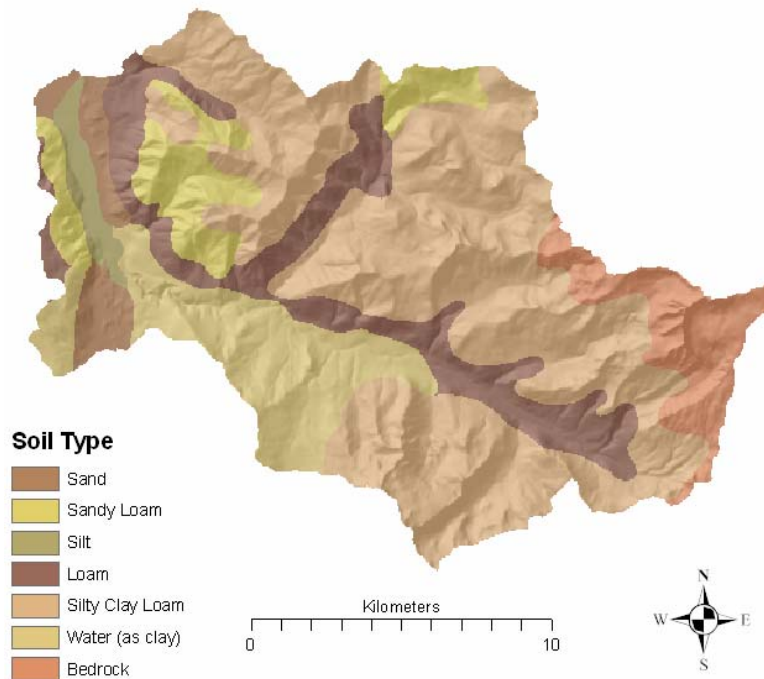


Figure 5: Soil type in the Middle Fork Nooksack River basin created using STATSGO soil data (Miller and White, 1998).

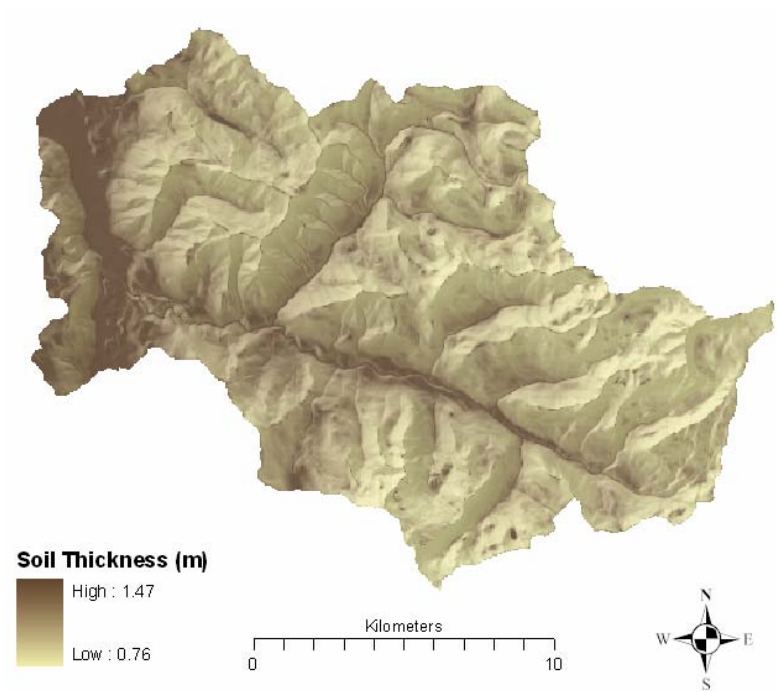


Figure 6: Soil thickness in the Middle Fork Nooksack River basin created using an ARCInfo AML.

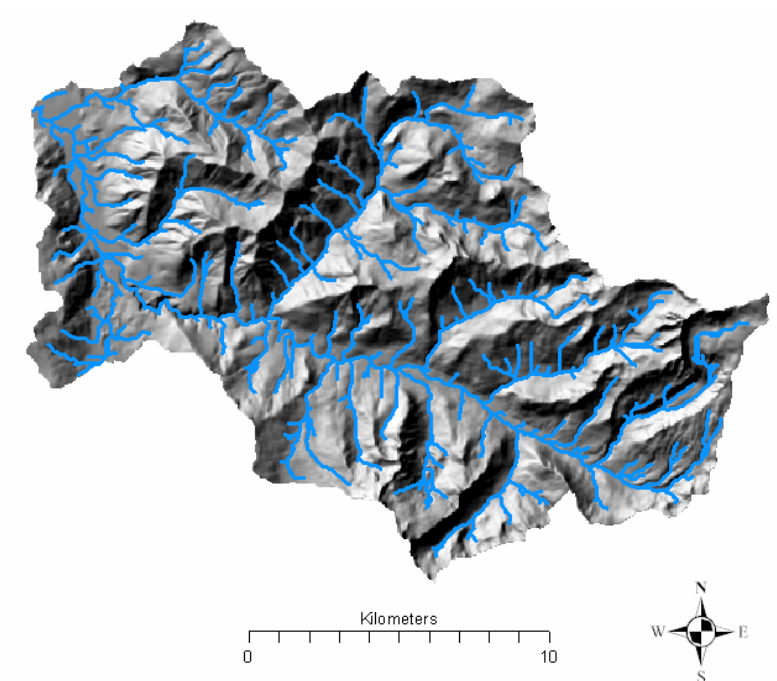


Figure 7: Stream network in the Middle Fork Nooksack River basin created using ARCInfo AML .

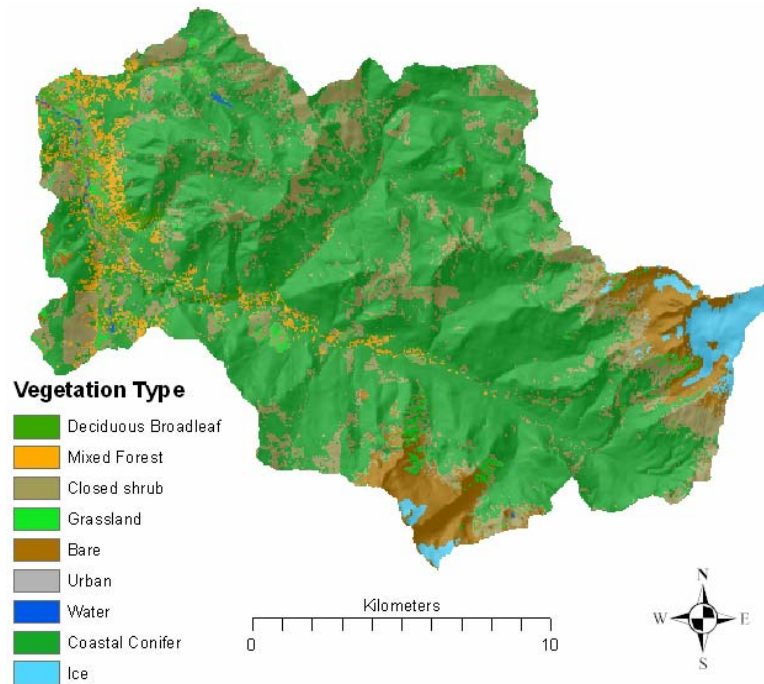


Figure 8: 2.6% glacier coverage in the Middle Fork Nooksack River basin (17% reduction in glacier size compared to 2002 coverage; predicted for year 2050 AD).

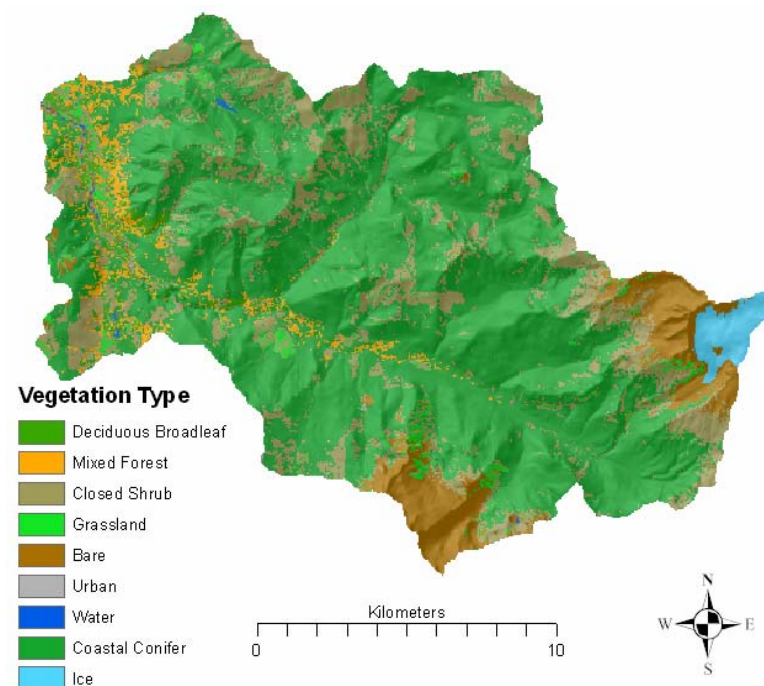


Figure 9: 1.6% glacier coverage in the Middle Fork Nooksack River basin (48% reduction in glacier size compared to 2002 coverage; predicted for year 2150 AD).

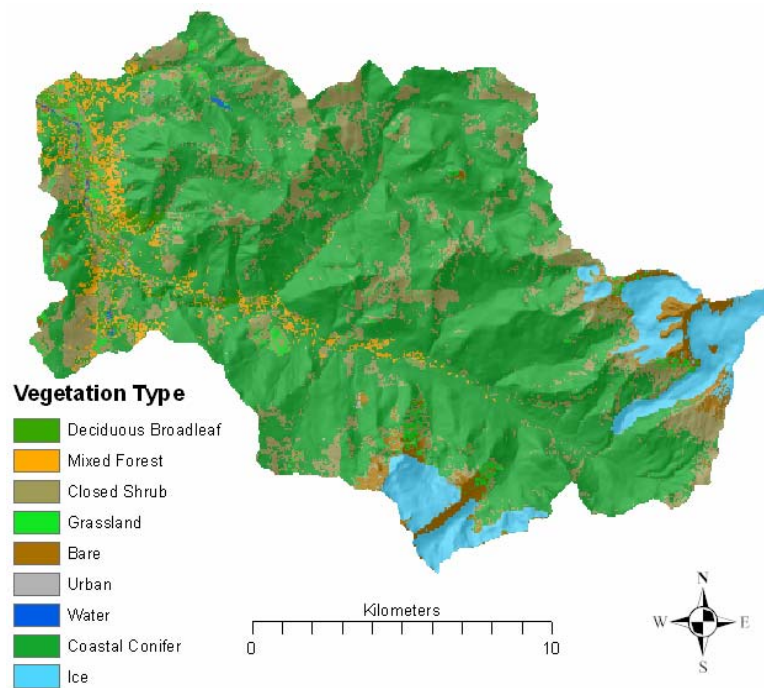


Figure 10: 7.6% glacier coverage in the Middle Fork Nooksack River Basin (144% increase in glacier size compared to 2002 coverage; estimated for the LIA maximum glacier extent).

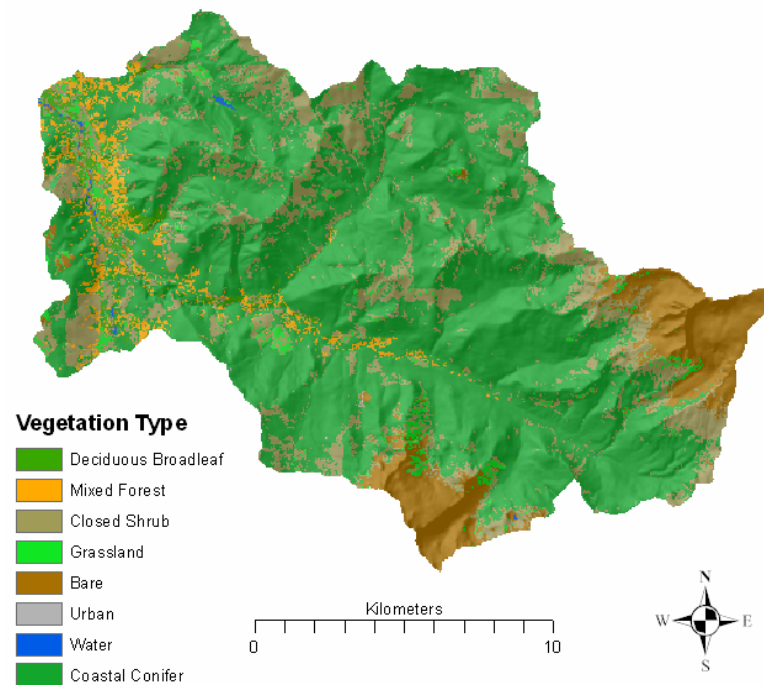


Figure 11: 0% glacier coverage in the Middle Fork Nooksack River basin.

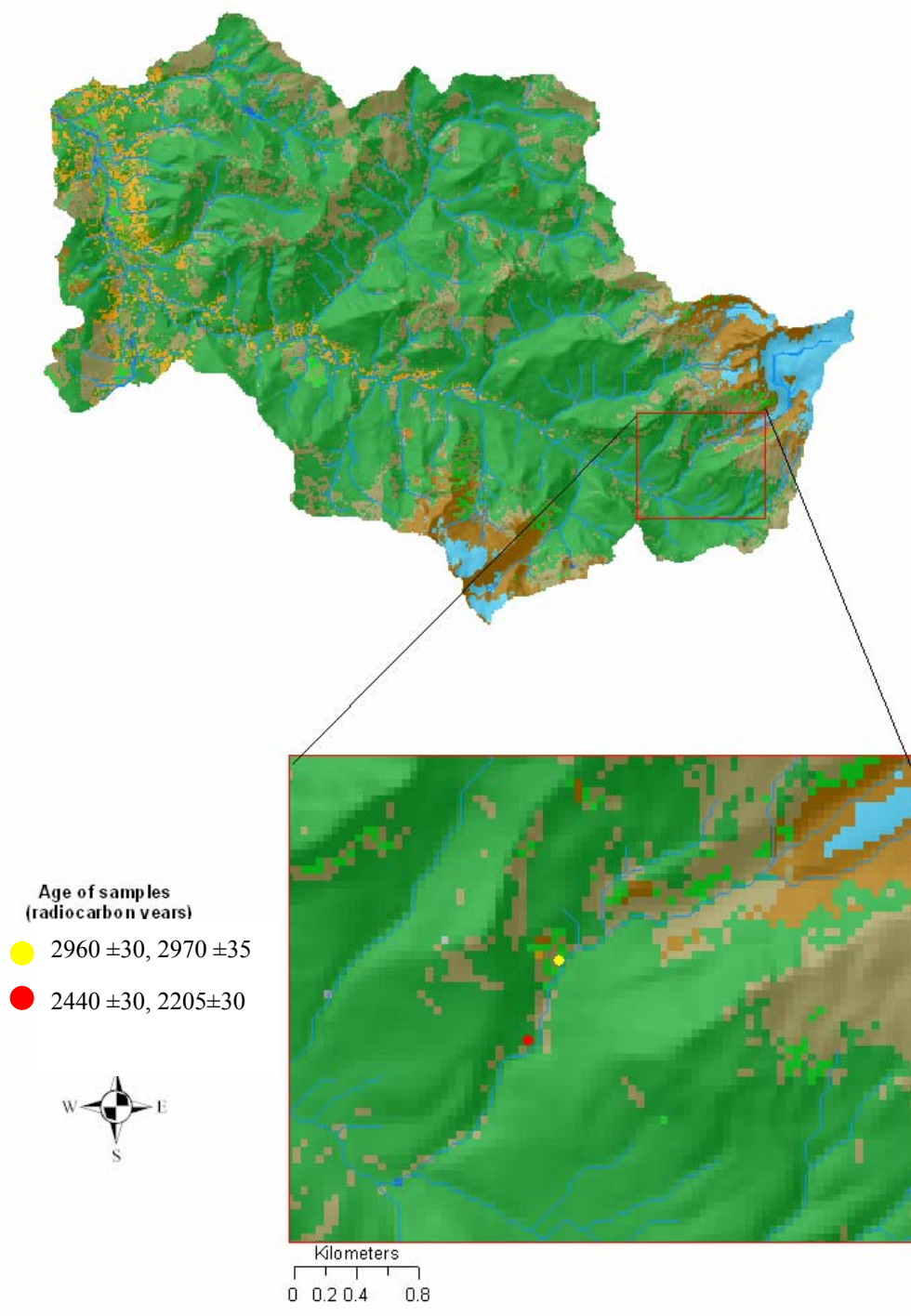


Figure 12: Location and ages of wood samples used for radiocarbon dating in the Middle Fork Nooksack basin.

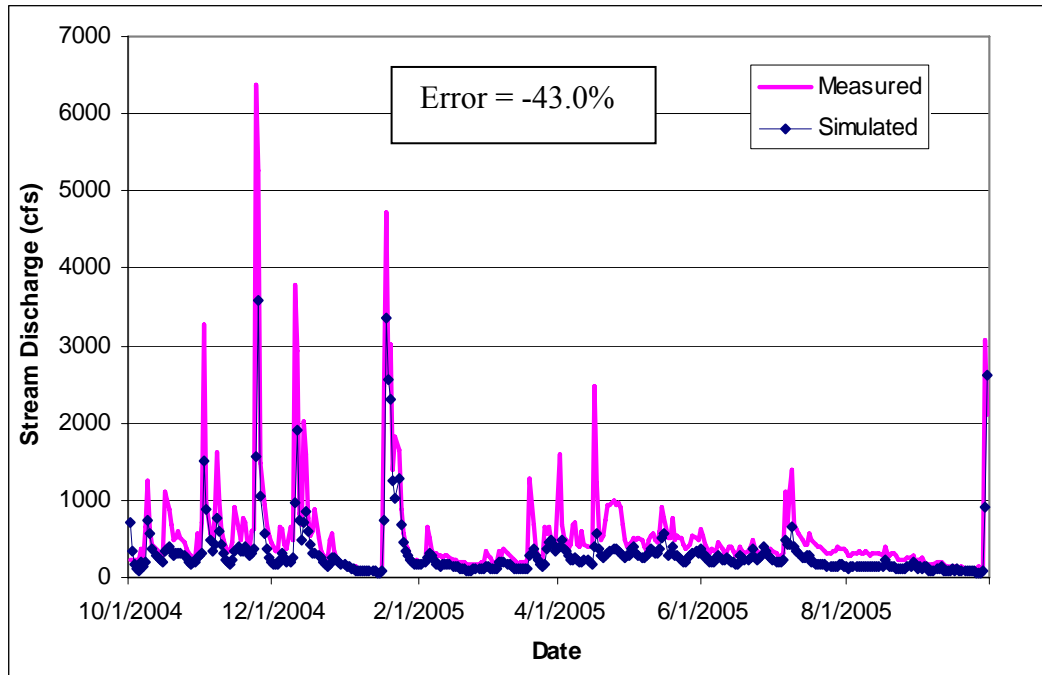


Figure 13: Daily mean discharge produced from the first DHSVM calibration simulation using default parameters.

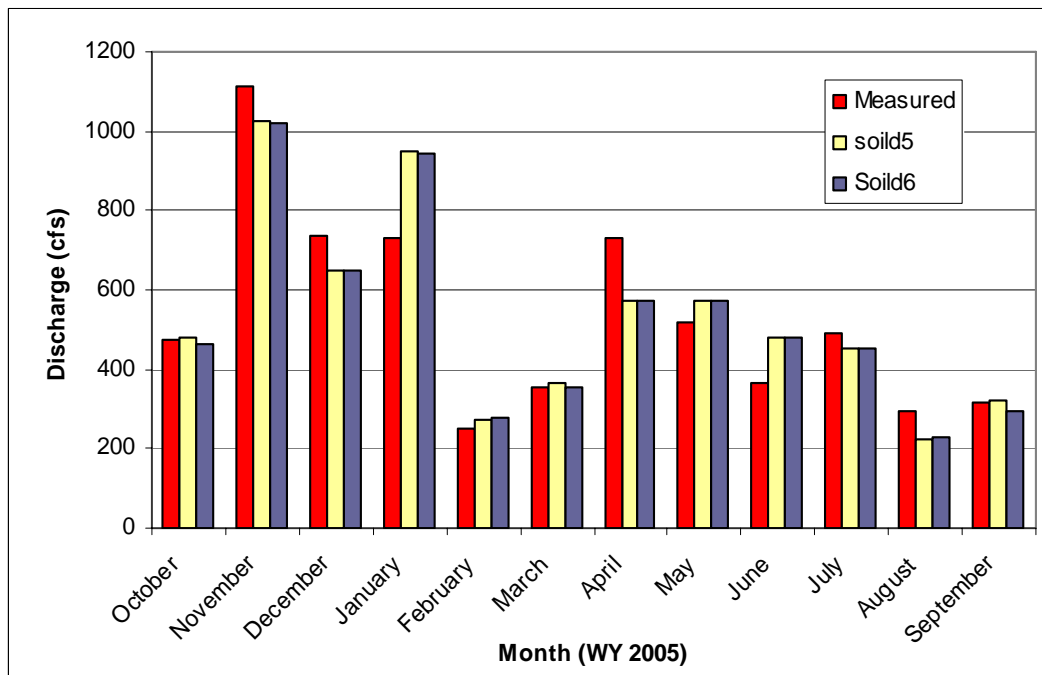


Figure 14: Monthly mean streamflow produced by calibration simulations using two different soil thicknesses (soild5 = 1.0-2.5 m, soild6 = 1.0-3.5 m).

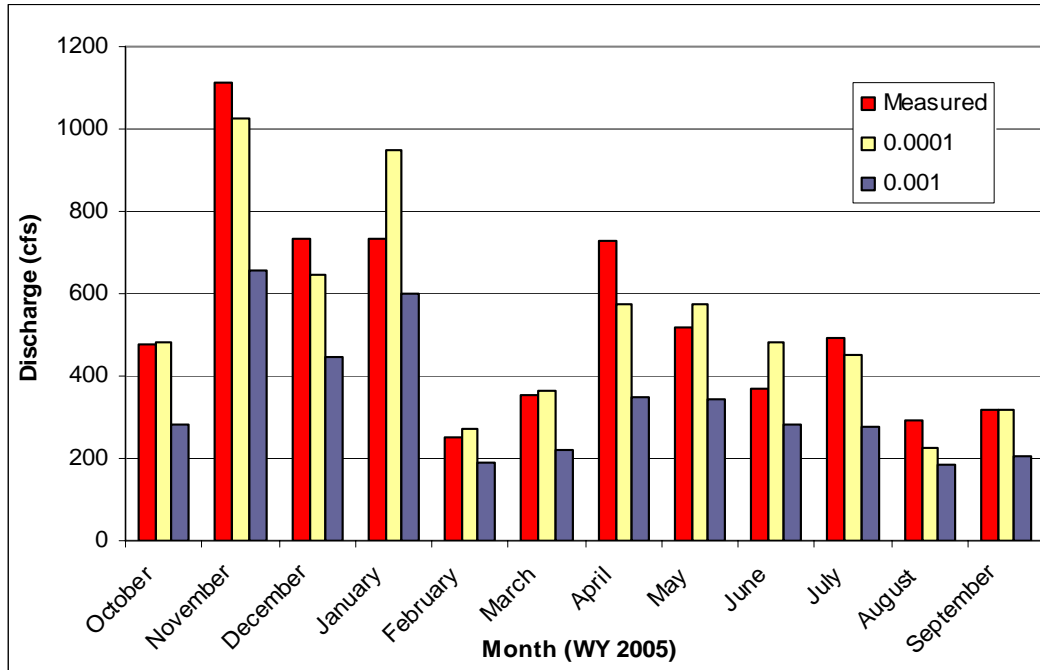


Figure 15: Monthly mean streamflow produced by calibration simulations using two different precipitation lapse rates (0.001 m/m and 0.0001 m/m).

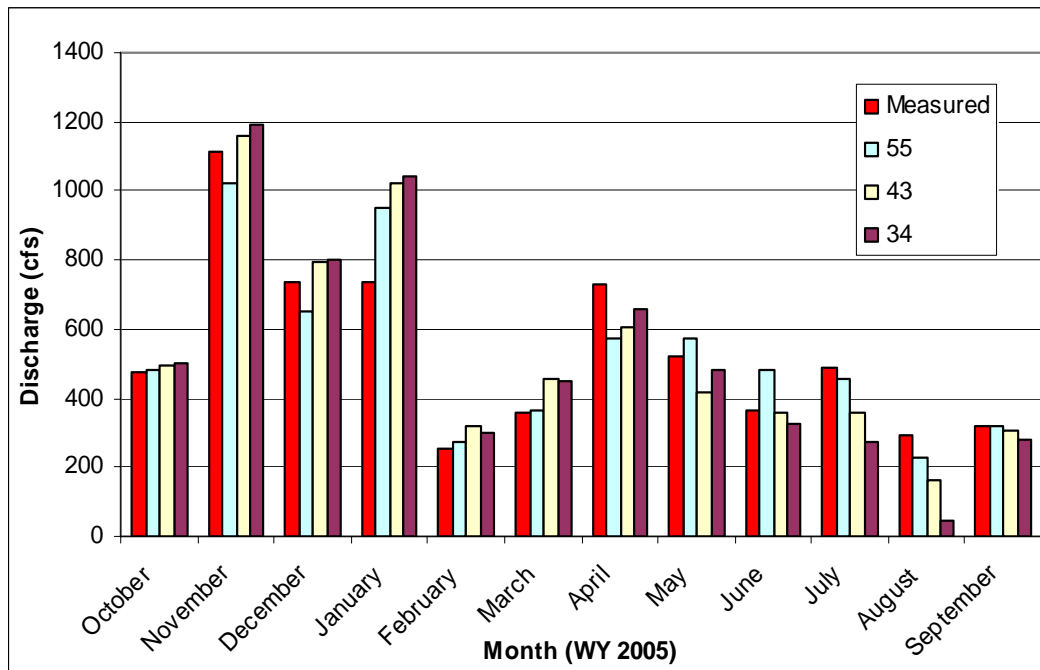


Figure 16: Monthly mean streamflow produced by calibration simulations using different temperature lapse rates (Simulation 34 = 0.0020 °C/km, Simulation 43 = variable, Simulation 55 = variable).

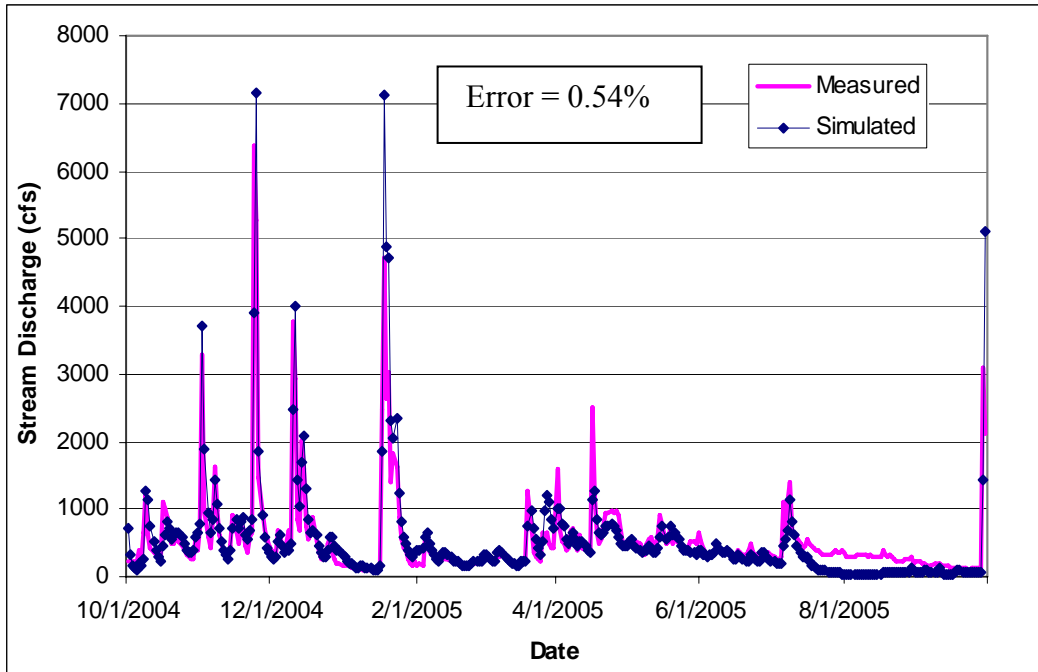


Figure 17: Daily mean discharge produced by calibration simulation before calibrating to snow-water equivalent.

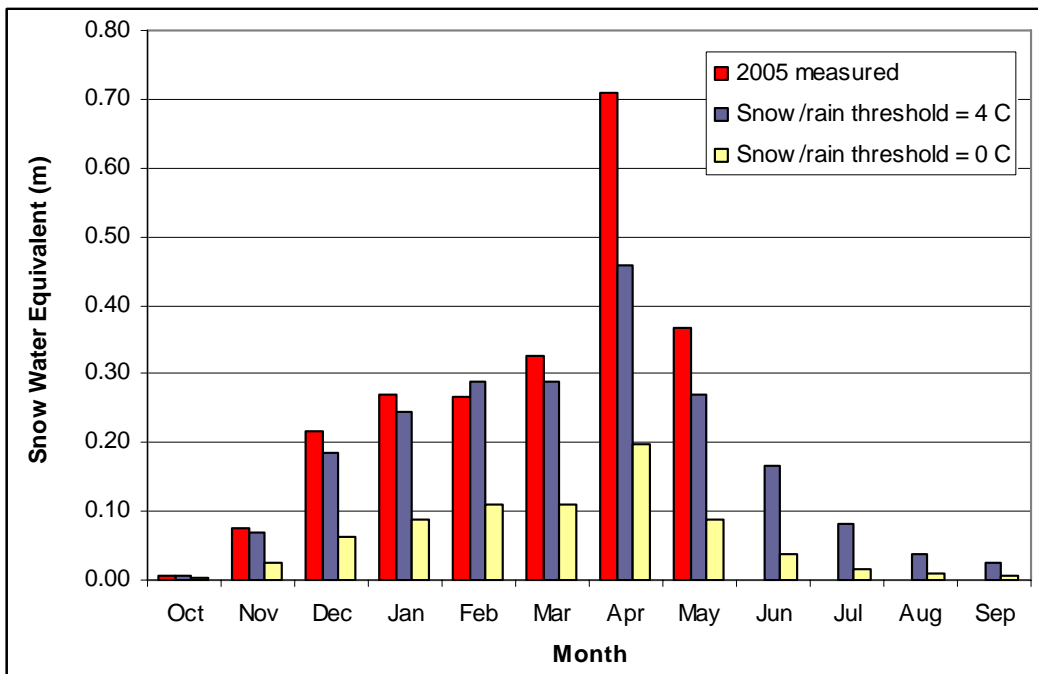


Figure 18: Measured and simulated average monthly snow-water equivalent at the Middle Fork SNOTEL station from calibration simulations using different values for snow/rain threshold temperature.

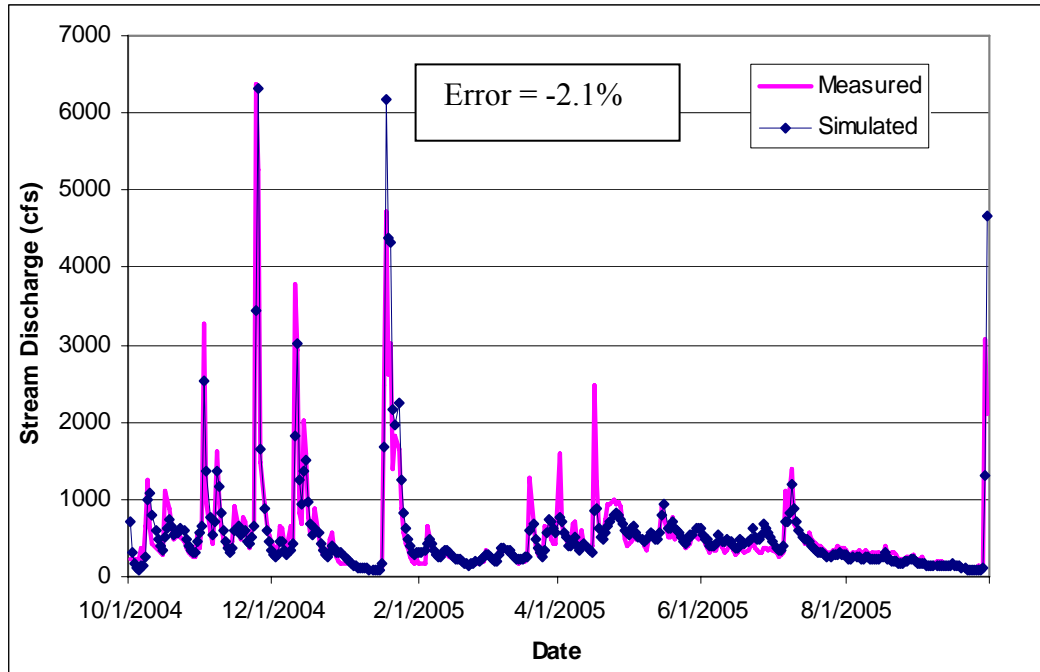


Figure 19: Daily mean discharge produced by calibration simulation for Water Year 2005. Snow/Rain threshold=4.0°C. Temperature lapse rate = variable (Nov-Jun Lapse rate=-0.006, Jul-Oct Lapse rate = -0.009), Precipitation Lapse rate =0.0001, K_L soil type 8=0.005, soil depth range = 1-2.5 m.

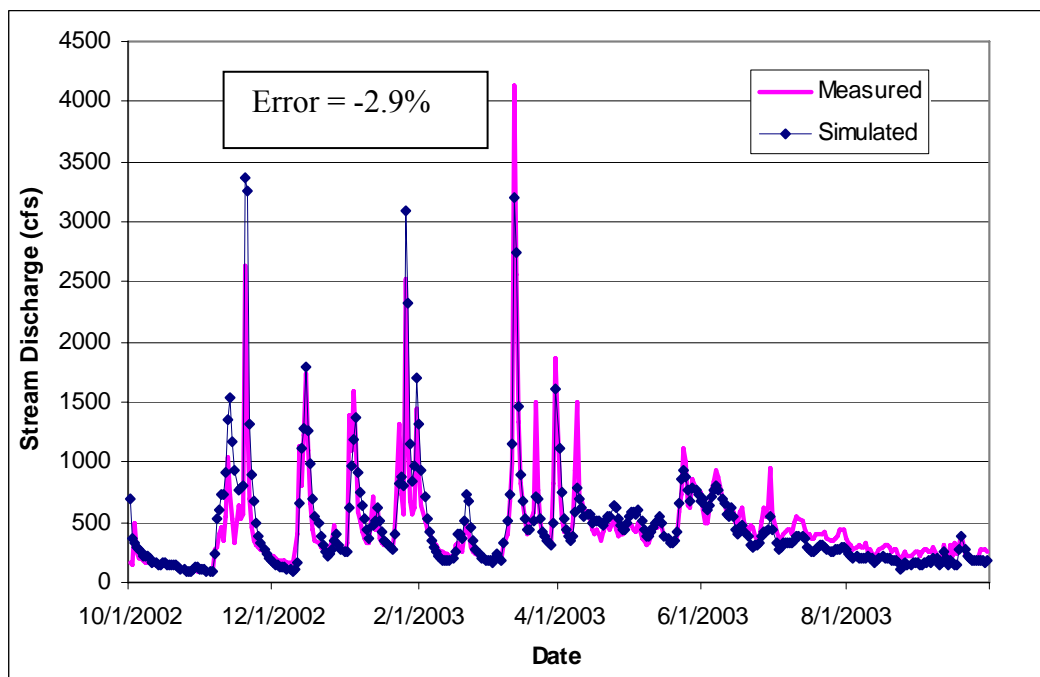


Figure 20: Daily mean discharge produced by validation simulation for water year 2003.

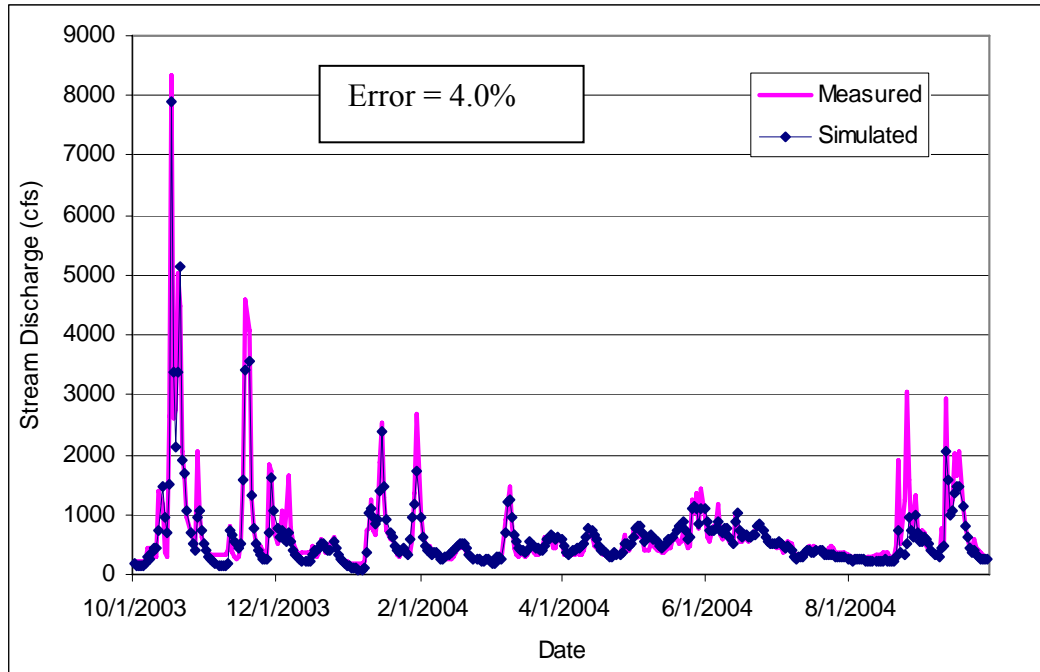


Figure 21: Daily mean discharge produced by validation simulation for Water Year 2004.

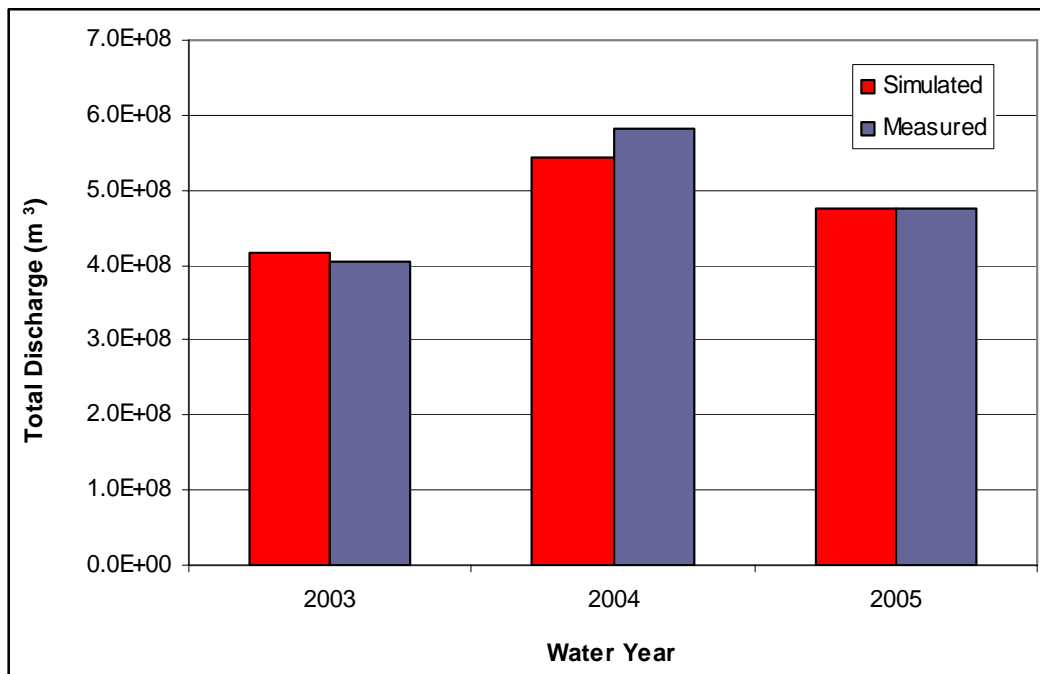


Figure 22: Total annual simulated and measured stream discharge for calibrated and validated application of DHSVM.

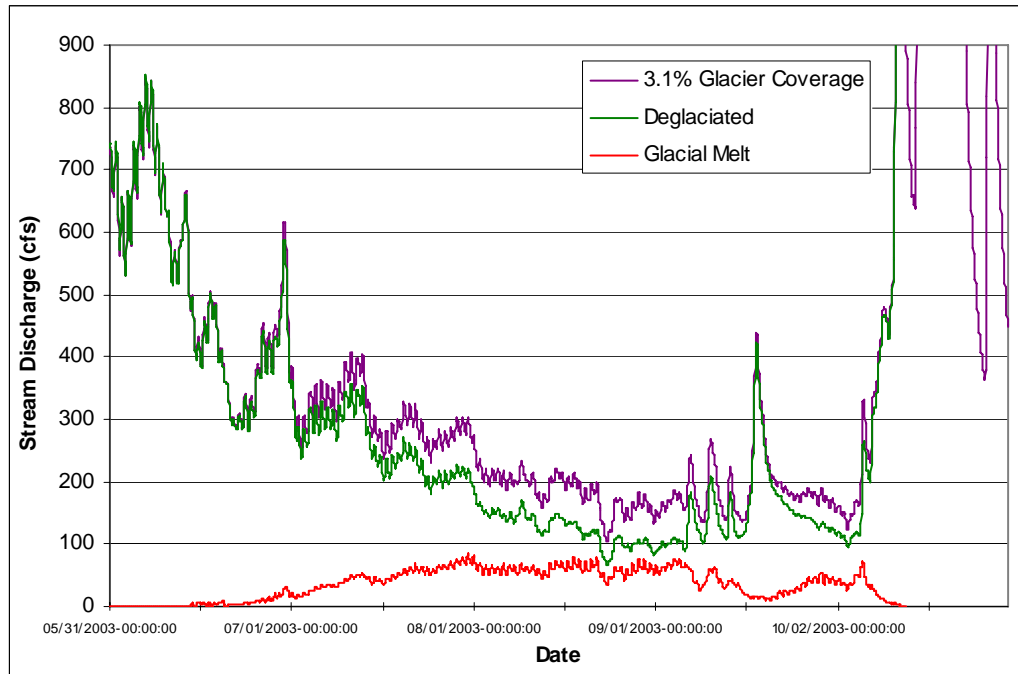


Figure 23: Glacial meltwater contribution produced by water year 2003 meteorological input with 2002 glacier coverage.

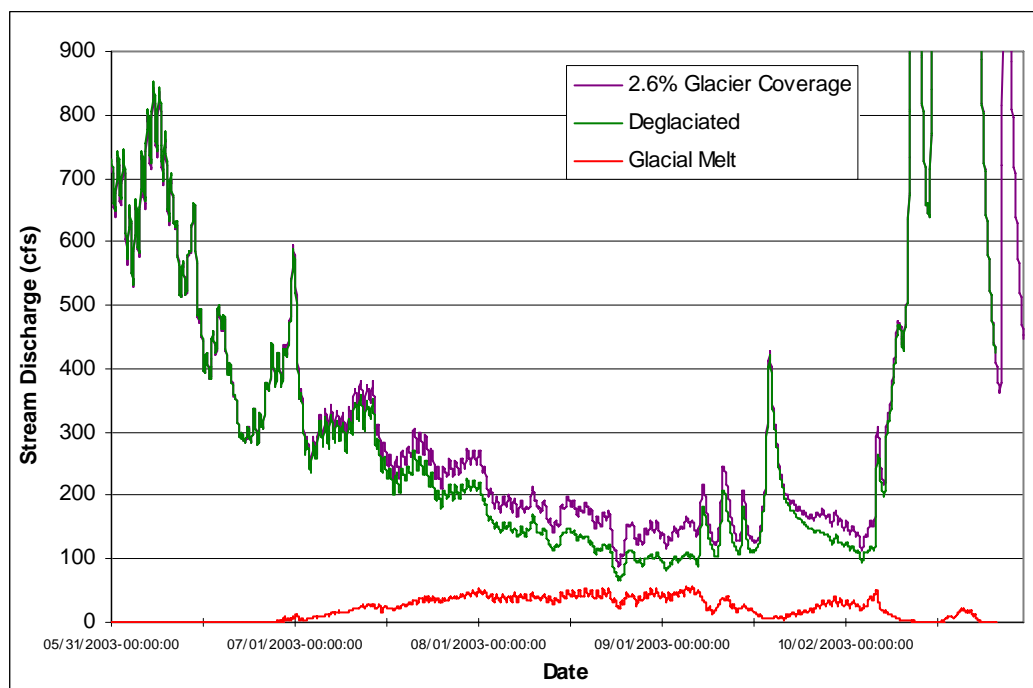


Figure 24: Glacial meltwater contribution produced by water year 2003 meteorological input with 17% reduction in glacier size (predicted for year 2050).

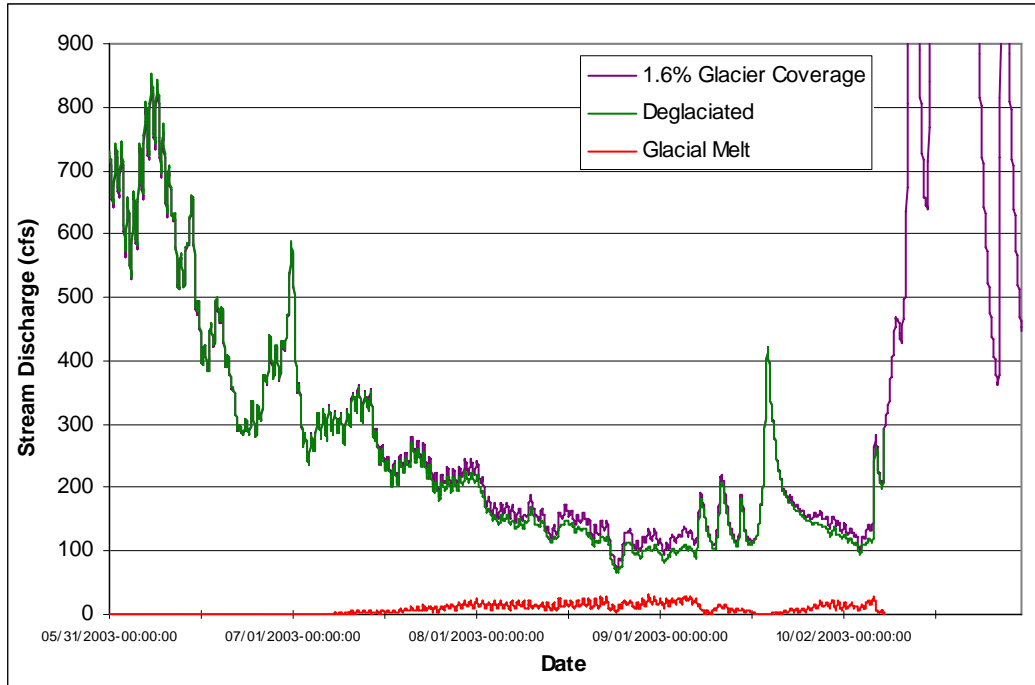


Figure 25: Glacial meltwater contribution produced by water year 2003 meteorological input with 48% reduction in glacier size (predicted for year 2150).

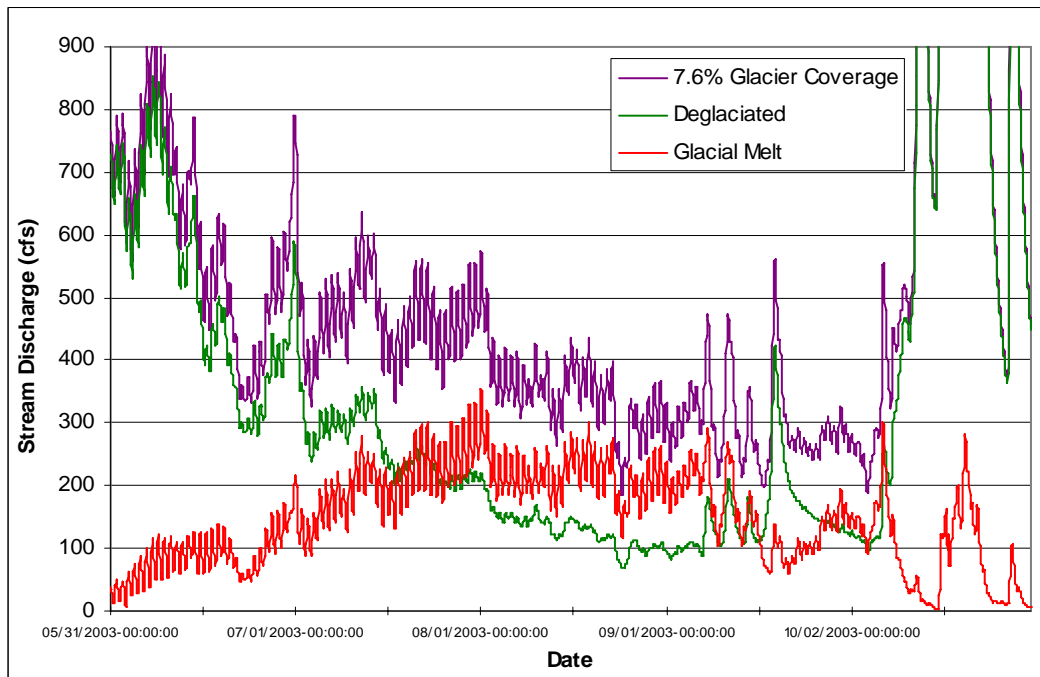


Figure 26: Glacial meltwater contribution produced by water year 2003 meteorological input with 144% increase in glacier size (estimated for LIA).

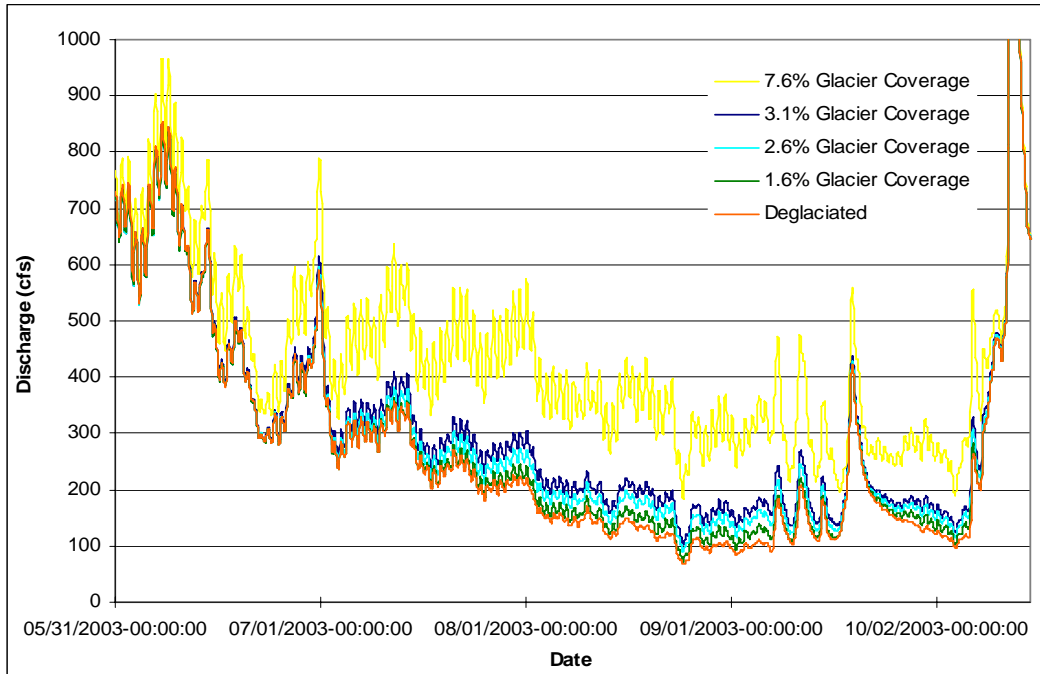


Figure 27: Summer stream hydrograph using present climate conditions and different glacier coverages.

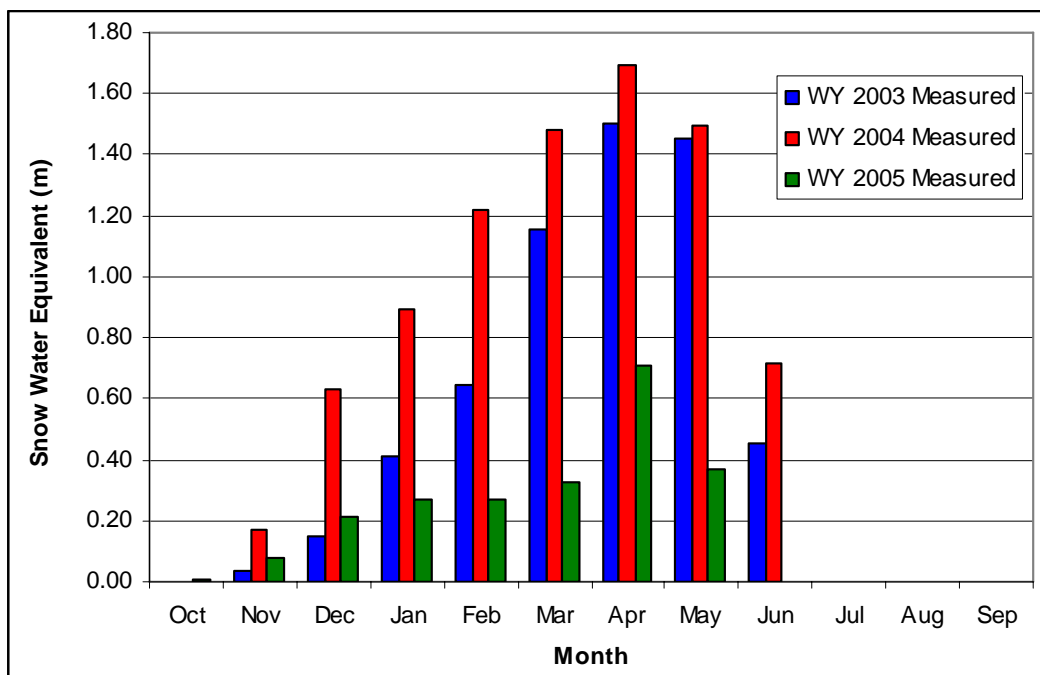


Figure 28: Measured monthly average snow-water equivalent at the Middle Fork SNOTEL station for the three years used as meteorological data input.

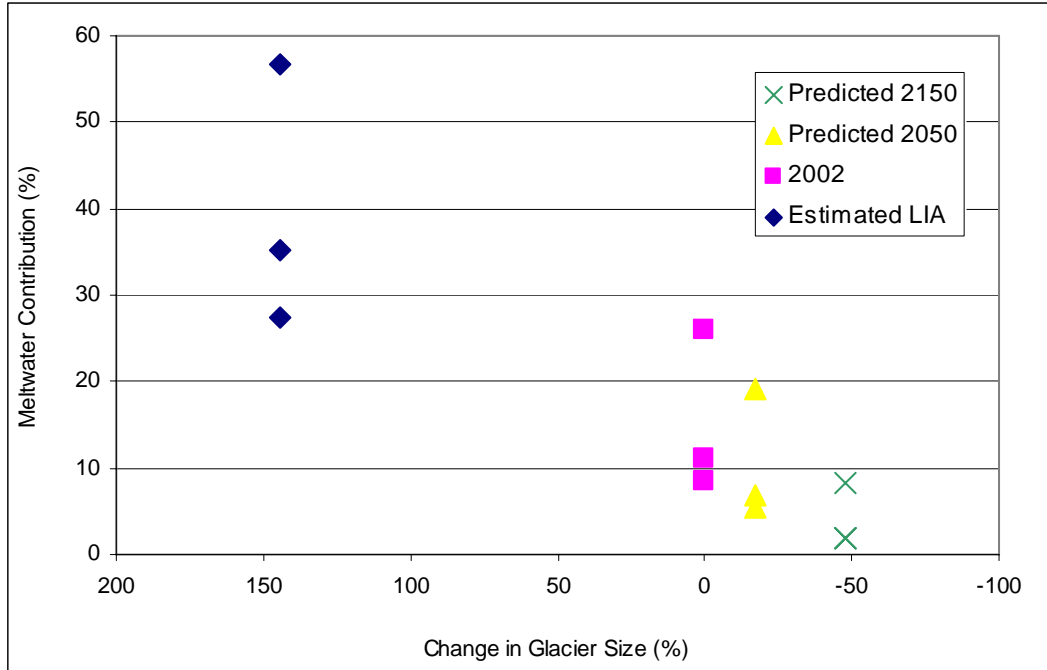


Figure 29: Summary of the non-linear relationship between glacier size and runoff. All simulations were based on present climate conditions and compared to 2002 glacier coverage.

Appendix A: DHSVM basin setup

1. CREATE A DEM GRID

1. Create a workspace. I created a folder on the C drive called MFdhsvm and created a folder within MFdhsvm for dems. (C:/MFdhsvm/dems)

2. Download and unzip Digital Elevation Models (DEMs).

I used the following DEMs in Washington State: Deming, Canyon Lake, Goat Mountain, Mt. Baker, Acme, Cavanaugh Creek, Twin Sisters, and Baker Pass.

I downloaded them from:

<http://duff.geology.washington.edu/data/raster/tenmeter/>

3. Convert DEM files to raster files

Open ArcMap→Arc Toolbox→Conversion Tools→To Raster→DEM to Raster

Input USGS DEM file: deming.dem

Output raster: C:/MFdhsvm/dems/deming

→OK

This will convert the DEM to a raster, and import the raster to ArcMap.

All DEMs have to be converted to raster files individually.

4. Mosaic DEMS

a. Set analysis environment

From Spatial Analyst dropdown menu→Options

Under general tab, Working directory: C:/MFdhsvm/dems.

Under Extent tab, Analysis extent: Union of Inputs

Under Cell size tab, Analysis cell size: Maximum of Inputs

→OK

b. Mosaic the DEMs using Raster Calculator

Open Spatial Analyst toolbar → raster calculator

Create the Mosaic expression in the text box:

<Nooksackdem>=mosaic ([deming], [CanyonLake], [etc.])

→Evaluate

c. Once DEMs are mosaicked, locate the new DEM in ArcCatalog and drag it into ArcMap.

5. Resample DEMs to 50 m by 50 m pixel resolution.

a. Set analysis environment (very important)

Open ArcToolbox→Data Management tools→Raster→Resample→environment

Under General Settings tab:

Present Workspace: (C:/MFdhsvm/dems)

Scratch Workspace (C:/MFdhsvm/dems)

Output coordinate system: Same as layer “Nooksackdem”

Output Extent: Same as layer “Nooksackdem”

Under Raster Analysis settings tab:

Cell size: 50
Mask: None
→OK

- b. Resample:
Input Raster: "Nooksackdem"
Output Raster: "dem50"
Cell size: 50
Resampling Technique: Nearest
→OK

Once the mosaicked raster is resampled to 50m resolution, Nooksackdem (10 m resolution) can be removed from ArcMap.

2. CREATE A WATERSHED MASK

1. Create another folder within the MFdhsvm folder. I titled mine "setup".

2. Fill sinks to even out the dem

Open hydrology/models toolbar→Fill Sinks
Input surface: dem50
Fill limit: <Fill_All>
Output raster: C:/MFdhsvm/setup/filldem
→OK

3. Perform flow direction on the filled DEM. This grid is necessary for determining the watershed boundary.

Open hydrology/models toolbar→Flow direction
Input surface: filldem
Output raster: C:/MFdhsvm/setup/flowdir
→OK

4. Perform flow accumulation. This grid is also necessary for determining the watershed boundary.

Open hydrology/models toolbar→Flow accumulation
Direction raster: flowdir
Output raster: C:/MFdhsvm/setup/flowacc
→OK

5. Set interactive properties to create a watershed boundary

Open hydrology/models toolbar→Interactive properties
Flow direction: flowdir
Flow accumulation: flowacc
→OK

6. Create the watershed boundary

Click the watershed button from the hydrology/models toolbar.

This is an interactive tool which will determine the boundary of the watershed based on the destination cell. I selected the point at which the Middle Fork converges with the main channel of the Nooksack River and ArcGIS determined which cells would eventually drain water to that point. I had to repeat the process a number of times before I was satisfied with the watershed boundary.

When a watershed is created, it may be a temporary file. To make it permanent, right-click on the watershed grid in ArcMap table of contents→Make Permanent→set source to the present workspace (C:/MFdhsvm/setup/watershed).

7. Create a watershed polygon

I created a watershed polygon that is used to clip the grids that are necessary input for DHSVM.

Open ArcToolbox→Conversion Tools→From Raster→Raster to Polygon

Input raster: C:/MFdhsvm/setup/watershed

Output polygon features: C:/MFdhsvm/setup/watershedpoly

→OK

8. Once the watershed polygon is created, it can be used to **clip the DEM** and hillshade (optional) **to the watershed**.

Set working environment:

Click Spatial Analysts toolbar→ Options

Working directory: C:/MFdhsvm/setup

Analysis mask: watershedpoly

Extent: watershedpoly

Cellsize: 50

From Spatial Analyst dropdown menu→raster calculator

Type the expression: sheddem=nooksackdem

→Evaluate

3. CREATE A LANDCOVER GRID

1. Download 2001 landcover grid from NOAA from

<http://www.csc.noaa.gov/crs/lca/pacificcoast.html>.

I downloaded the coverage for the entire west coast.

The landcover file is already an ESRI grid, so it does not need to be converted. The PCS may be different than that for the DEM, but ArcGIS should be able to project the grid on the fly.

2. Resample grid to 50 by 50 m resolution.

Open ArcToolbox→Data management Tools→Raster→Resample

Set the analysis environment (very important):

Under General Settings tab:

Present Workspace: (C:/MFdhsvm/setup)

Scratch Workspace (C:/MFdhsvm/setup)

Output coordinate system: Same as layer “Nooksackdem”

Output Extent: Same as layer “Nooksackdem”

Under Raster Analysis settings tab:

Cell size: 50

Mask: None

→OK to close environments setting

Input raster: landcover

Output raster: landcover50

Output cell size: 50

Resampling technique: nearest neighbor

→OK

3. Clip landcover grid to watershed boundary.

Set analysis environment:

Click Spatial Analysts toolbar→ Options

Working directory: C:/MFdhsvm/setup

Analysis mask: watershedpoly

Extent: watershedpoly

Cellsize: 50

From Spatial Analyst dropdown menu→raster calculator

Type the expression: shedcover=landcover50

→Evaluate

4. Reclassify NOAA vegetation classifications to DHSVM classifications

Open ArcToolbox→Spatial Analyst→Reclass→Reclassify

Set general and raster analysis environments

Input Raster: landshed

Output Raster: reclassveg

Reclass Field: Value

Then:

NOAA	NOAA	DHSVM	DHSVM
2	High Intensity Developed	13	Urban
3	Low Intensity Developed	13	Urban
5	Grassland	10	Grassland
6	Deciduous Forest	4	Deciduous Broadleaf
7	Evergreen Forest	15	Coastal Conifer
8	Mixed Forest	5	Mixed Forest
9	Scrub/Shrub	8	Closed Shrub
10	Palustrine Forested Wetland	4	Deciduous Broadleaf

11	Palustrine Scrub/Shrub Wetland	8	Closed Shrub
12	Palustrine Emergent Wetland	10	Grassland
16	Unconsolidated Shore	12	Bare
17	Bare land	12	Bare
18	Water	14	Water
19	Palustrine Aquatic Bed	14	Water
22	Ice	20	Ice

4. CREATE VARIABLE GLACIER GRIDS

1. Map out glacial moraines. I used a stereo pair of aerial photos to map moraines.

2. Determine retreat rate of glacier(s) (see section 4.1.3).

3. Download digital aerial photos and bring them into ArcMap. I downloaded photos from <http://gis.ess.washington.edu/data/raster/doqs.html>, and merged them using the ‘mosaic’ command in Raster Calculator (see ‘mosaic DEMs’).

4. Create a new feature in ArcCatalog

Open ArcCatalog → Open your workspace (I created a new workspace called ‘glacier coverages’ in the ‘setup’ folder → click new → shapefile → Name: glacier2050, Feature Type: polygon.

Drag the new shapefile into ArcMap table of contents along with the aerial photos and present vegetation layer.

5. Edit the new shapefile

In ArcMap click Editor → start editing → select glacier2050 → Task: create new feature, Target: glacier2050.

Click on the pencil; begin digitizing the past or future glacier coverages by creating polygons that will be merged with the present vegetation grid. I used the measuring tool, the present vegetation grid, and the air photos to aid in digitizing. When creating smaller glaciers, the polygons will be reclassified to ‘Bare’ soil type and then merged with the vegetation grid.

6. Convert the shape file to a raster (see ‘convert soil polygon to raster’ below)

7. Reclassify the new raster to vegetation type 12 (bare) or type 20 (Ice) (See ‘Reclassify NOAA vegetation classifications to DHSVM classifications’ above).

8. Merge the reclassified raster with the original landcover grid.

In the Spatial Analyst drop down menu, set options.

Open Raster Calculator → Type: Glacier2050 = merge ({reclassified raster}, {veg grid}) → Evaluate

Glacier2050 is now the new vegetation grid representing smaller glaciers.

5. CREATE A SOIL TEXTURE GRID

1. Download soil texture coverage from STATSGO for Whatcom County, WA from http://www.essc.psu.edu/soil_info/etc/statsgolist.cgi?statename=Washington

I created a new folder within C:/MFdhsvm called soils. Save the file (wa.e00) in this file.

2. Convert file. This is a GIS export file that has to be converted in ArcCatalog.

Open ArcCatalog→Conversion Tools→Import from Interchange File

Input file: C:\MFdhsvm\soil\wa.e00\wa.e00

Output dataset: C:\MFdhsvm\soil\wa

The file will now appear in ArcCatalog and can be dragged into ArcMap.

The PCS may be different than that for the DEM, but ArcGIS should be able to project the grid on the fly.

3. Convert soil polygon to raster.

Open ArcToolbox→Conversion Tools→To Raster→Feature to Raster

Set analysis environments by clicking on the Environments button

Under General Settings tab:

Present Workspace: (C:/MFdhsvm/soils)

Scratch Workspace (C:/MFdhsvm/soils)

Output coordinate system: Same as layer “Nooksackdem”

Output Extent: Same as layer “Nooksackdem”

Under Raster Analysis settings tab:

Cell size: 50

Mask: None

OK to close environments setting

Input features: wa polygon

Field: MUID

Output raster: C:\MFdhsvm\soil\wa.e00\wa\soilgrid

Output cell size: 50

→OK

Remove wa polygon from ArcMap

4. Clip soil grid to watershed

Set analysis environment:

Click Spatial Analysts toolbar→ Options

Working directory: C:/MFdhsvm/soils

Analysis mask: watershedpoly

Extent: watershedpoly

Cellsize: 50

From Spatial Analyst dropdown menu→raster calculator

Type the expression: soilshed=soilgrid
 →Evaluate

Soil classifications are as follows:

MUID	Description	MUID	Description
1*	Sand	10	Sandy Clay
2	Loamy Sand	11	Silty Clay
3*	Sandy Loam	12	Clay
4	Silty Loam	13	Organic (as loam)
5*	Silt	14*	Water (as clay)
6*	Loam	15*	Bedrock
7	Sandy Clay Loam	16	Other (as SCL)
8*	Silty Clay Loam	17	Muck
9	Clay Loam	18	Talus

* Soil classifications in the Middle Fork Nooksack basin

6. CREATE SOIL DEPTH AND STREAM NETWORK GRIDS

I created the soil depth and stream network grids using Arc in the spatial analysis lab (AH 16) using the following methods:

1. Create a workspace

Create a new folder: C:/TEMP/soild

Copy the watershed grid (watershed), the clipped dem (sheddem) and amlscripts from the DHSVM tutorial into the “soild” folder.

Check the computer to ensure that it has a Java Runtime Environment (JRE). If it doesn’t, download Java software from www.sun.com.

To check for JRE, open Arc and type:

Arc: &sys java -version

If the JRE is installed, you should get:

Java version “1.4.2_04”

Java [TM] 2 Runtime Environment, Standard Edition (build 1.4.2_04-b04)

Java HotSpot[TM] Client VM (build 1.4.2_04-b04, mixed mode).

The watershed mask values must be defined as inbasin=1 and outside basin=NODATA. Otherwise the AML will create a stream network for the entire raster. You can check the values in ArcMap by opening the DEM properties dialogue.

Before running the AML, make sure to change the path to AddAat2.class from with the createstreamnetwork AML. If this step is skipped, the AML will encounter an error, but will continue to run anyway. It will produce zeros within the streamnetwork.dat for slope, segorder, etc. and DHSVM cannot use this file.

I simply opened the AML, used the ‘find’ tool to locate the path and changed the path to:
&sys java -classpath ../soild/amlscripts/ AddAat2 %streamnet%

2. Run the AML

Open ARC.

Type:

ARC: &workspace C:/TEMP/soild

ARC: &watch aml.watch

ARC: &amspath C:/TEMP/soild/amlscripts

ARC: &run createstreamnetwork sheddem watershed mf_soild mf_streams MASK 220000
0.76 1.5

The last three numbers are variables representing the minimum contributing area before a channel begins, the minimum soil depth, and maximum soil depth (in meters).

7. CREATE A SERIES OF SHADING MAPS

1. Create a workspace

Create a new folder: C:/TEMP/shadow

Copy the clipped dem (sheddem) into this folder using ArcCatalog. The solar AML (process_solar1 is not available in the amlscripts folder in the DHSVM tutorial, but can be found in the amlscripts folder on the attached cd). This file should also be copied into the shadow folder. Process_solar.aml requires 3 “C” files to run. I compiled these using the ‘lcc’ compiler in the Computer Science department with the help of Matt Paskus. The compiled files which are make_dhsvm_shade_maps.exe, skyview.exe, and average_shadow.exe, can also be found on the attached cd. Copy these files into the ‘shadow’ file.

2. Run the AML

Type:

Arc: &workspace C:/TEMP/shadow

Arc: &watch aml.watch

Arc: &amspath C:/TEMP/shadow/amlscripts

Arc: &r process_solar1 middlefork sheddem 1 0.0

Arc: quit

The basin name is “middlefork” and the elevation grid is “sheddem”. The last two numbers represent the model timestep and GMT offset, respectively.

The AML command “rm” is not recognized in Windows. I transferred the shadow maps to Horton anyway, and renamed each file (ex: ‘Shadow.01.hourly.bin’ is renamed ‘shadow.01.bin’).

8. EXPORT DEM, SOIL TYPE, SOIL THICKNESS, VEGETATION, AND WATERSHED FILES AS ASCII GRIDS

I created a new file for each conversion and copied the GIS grid to be converted into the file.

I then convert all the NoData values in the grids to something that DHSVM recognizes (e.g., water=14) and converted the grids to ascii format.

Example:

For the watershed grid, Type:

Arc: &workspace C:TEMP/watershed (with “watershed” grid)

Arc: grid

GRID: watershed.asc = gridascii(con(isnull(watershed),14,watershed))

GRID: q

9. CONVERT ASCII GRIDS TO BINARY

I converted the ascii grids (soilclass.asc, vegclass.asc, and mask.asc) to binary files on Horton using “myconvert” in the input file.

The correct variable type for each grid is as follows:

Mask, landcover, soil type: unsigned character or “uchar”

Dem, soildepth: float

Example (for mask, landcover, soil type):

```
horton > ./myconvert ascii uchar mask.asc mask.bin 375 496
```

Example (for dem, soildepth):

```
horton > ./myconvert ascii float DEM.asc DEM.bin 375 496
```

Where:

```
horton> ./myconvert source_format target_format source_file target_file number_of_rows  
number_of_columns
```

10. CREATE A FINAL STREAM MAP AND STREAM NETWORK FILE

I created these files on Horton using “assign”. The files stream.network.dat and stream.map.dat were created during step #5 (stream network grid). mf.stream-net.dat and mf.stream-map.dat are the final map and network files.

Example:

```
horton> ./assign stream.network.dat stream.map.dat mf.stream-net.dat mf.stream-map.dat
```

11. LOCATE THE STREAM GAUGE FOR DHSVM CALIBRATION.

The stream gage location in DHSVM is based on the location of the end of a stream segment generated in the stream network aml, not the actual location of the gage. Open ArcMap.

Drag into a new, empty map: sheddem and the streams arc. Locate the position of the stream gauge using the coordinate indicators in the lower right corner of the screen, or plot

the location of the stream gauge using “Tools” and “add X Y data”. The output segment is the segment that terminates the closest to the stream gauge location. Stream discharge is not at a pixel, it is at the end of a selected stream segment. After the stream gauge is located, click on the stream segment nearest the gauge to determine the stream segment ID #. Record the segment number/value. In the stream network file, type ‘SAVE’ next to the appropriate stream segment.

12. SET INITIAL CONDITIONS FOR DHSVM CALIBRATION

1. Create initial channel state files:

Unix: % awk' {print \$1, 0.1} mf.stream_net.dat> channel.state.9.30.2003.00.00

2. Create model state files

I used initialstate.txt that is found in the dshvm tutorial and changed the path, date, and # of rows and columns.

Then:

Horton: MakeModelStateBin InitialState.txt

This creates the initial Interception, Snow, and Soil state files for the date that is specified in the initialstate.txt file. The date indicates the beginning of the model simulation.

13. RUN THE MODEL

From the mfork directory (horton/carrie/dshvm/mfork>)

horton> DHSVM input.mfork

Appendix B: All simulations performed for model calibration and validation.

	Simulation	Water Year	initial State	Met Stations	% error	Parameters
3 stations	0	2005	Dry	Elbow, Wells, MF	NA	NA
	1	2002	End of simulation 1	Elbow, Wells, MF	-39.18%	Default parameter settings
	2	2002	End of simulation 1	Elbow, Wells, MF	-34.95%	Changed lateral hydraulic conductivity for dominant soil type (8) (from 0.01 to 0.005)
	3	2002	End of simulation 1	Elbow, Wells, MF	-41.80%	Changed lateral hydraulic conductivity for all soil types (from 0.01 to 0.005)
	4	2002	End of simulation 1	Elbow, Wells, MF	-41.90%	Changed soil thickness range from 1-2.5 to 1-3.5m
	5	2002	End of simulation 1	Elbow, Wells, MF	-40.34%	Doubled precipitation lapse rate (from 0.0012 to 0.0024)
	7	2002	End of simulation 1	Elbow, Wells	-40.34%	Doubled precipitation lapse rate (from 0.0012 to 0.0024)
	8	2002	End of simulation 1	Elbow, Wells	-35.70%	4x precipitation lapse rate (0.0048)
	11	2002	End of simulation 1	Elbow, Wells	-32.52%	5x precipitation lapse rate (0.0060)

Table B1: Simulations performed using all three meteorological data sets: Elbow Lake, Wells Creek, and Middle Fork SNOTEL stations.

	Simulation	Water Year	initial State	Met Stations	% error	Parameters
1 Station	9	2002	End of simulation 1	Elbow Lake	42.19%	Default parameter settings, Elbow Lake only
	6	2002	End of simulation 1	Elbow Lake	49.24%	2x precipitation lapse rate (0.0024)
	10	2002	End of simulation 1	Elbow Lake	41.91%	Changed soil thickness range from 1-2.5 to 1-3.5m
	12	2002	End of simulation 1	Elbow Lake	39.60%	1/2x precipitation lapse rate (0.0006)

	13	2002	End of simulation 1	Elbow Lake	37.74%	1/4x precipitation lapse rate (0.0003)
	14	2002	End of simulation 1	Elbow Lake	41.99%	default precipitation lapse rate, K_L of soil type 8 0.005
	15	2002	End of simulation 1	Elbow Lake	37.33%	P-lapse rate 0.0003, Soild 6 (1-3.5m), K_L of soil type 8 0.005
	16	2002	End of simulation 1	Elbow Lake	37.57%	P-lapse rate 0.0003, Soild 6 (1-3.5m), K_L of soil type 8 0.002
	17	2002	End of simulation 1	Elbow Lake	35.13%	P-lapse rate 0, Soild 6 (1-3.5m), K_L of soil type 8 0.002
	19	2005	End of simulation 1	Elbow Lake	21.46%	P-lapse rate 0, Soild 6 (1-3.5m), K_L of soil type 8 0.002

Table B2: Simulations performed using only Elbow Lake SNOTEL station (Continued from above).

	Simulation	Water Year	initial State	Met Stations	% error	Parameters
Middle Fork SNOTEL only	22	2005	End of simulation 1	Middle Fork	-43.03%	Default parameter settings, Middle Fork only
	23	2005	End of simulation 1	Middle Fork	-43.28%	K_L of soil type 8 0.005
	24	2005	End of simulation 1	Middle Fork	-55.32%	K_L of soil type 8 0.005, 2X precipitation lapse rate (0.0024)
	25	2005	End of simulation 1	Middle Fork	-40.99%	K_L of soil type 8 0.005, 1/2X temperature lapse rate (0.00325)
	26	2005	End of simulation 1	Middle Fork	-40.50%	K_L of soil type 8 0.02, 1/2X temperature lapse rate (0.00325)
	27	2005	End of simulation 1	Middle Fork	-42.64%	K_L of soil type 8 0.04, default temperature lapse rate
	28	2005	End of simulation 1	Middle Fork	-48.41%	2X temperature lapse rate (0.013)
	29	2005	End of simulation 1	Middle Fork	-43.42%	default settings, soild6

30	2005	End of simulation 1	Middle Fork	3.67%	all default except precipitation lapse rate = 0.000
31	2005	End of simulation 1	Middle Fork	0.67%	P-lapse rate =0.0001, T-lapse rate=0.0040, K _L soil8=0.05, soild5
32	2005	End of simulation 1	Middle Fork	0.13%	P-lapse rate =0.0001, T-lapse rate=0.0065, K _L soil8=0.05, soild5
33	2005	End of simulation 1	Middle Fork	0.69%	P-lapse rate =0.0001, T-lapse rate=0.0040, K _L soil8=0.005, soild5
34	2005	End of simulation 1	Middle Fork	0.48%	P-lapse rate =0.0001, T-lapse rate=0.0020, K _L soil8=0.005, soild5
35	2005	End of simulation 1	Middle Fork	0.54%	P-lapse rate =0.0001, T-lapse rate=0.0020, K _L soil8=0.005, soild5, snow threshold =0.25
36	2005	End of simulation 1	Middle Fork	1.65%	P-lapse rate =0.00005, T-lapse rate=0.0020, K _L soil8=0.005, soild5, snow threshold =0.25
37	2005	End of simulation 1	Middle Fork	0.61%	P-lapse rate =0.0001, T-lapse rate=0.0020, K _L soil8=0.005, soild5, snow threshold =0.00
38	2005	End of simulation 1	Middle Fork	3.88%	P-lapse rate =0.0001, T-lapse rate=0.0100, K _L soil8=0.005, soild5, snow threshold =0.00
39	2005	End of simulation 1	Middle Fork	41.43%	P-lapse rate =0.0010, T-lapse rate=0.0100, K _L soil8=0.005, soild5, snow threshold =0.00
40	2005	End of simulation 1	Middle Fork	39.00%	Same as above except veg 20 = glacier, not Ice
41	2005	End of simulation 1	Middle Fork	4.39%	P-lapse rate =0.0001, T-lapse rate=0.0020, K _L soil8=0.005, soild5, snow threshold =0.00
42	2005	End of simulation 1	Middle Fork	NA	incomplete model run
43	2005	End of simulation 1	Middle Fork	1.29%	P-lapse rate =0.0001, T-lapse rate=variable2, K _L soil8=0.005, soild5
44	2005	End of simulation 1	Middle Fork	3.34%	P-lapse rate =0.0001, T-lapse rate=variable3, K _L soil8=0.005, soild5
45	2005	End of simulation 1	Middle Fork	3.16%	P-lapse rate =0.0001, T-lapse rate=variable4, K _L soil8=0.005, soild5

46	2005	End of simulation 1	Middle Fork	2.81%	P-lapse rate =0.0001, T-lapse rate=variable5, K _L soil8=0.005, soild5
47	2005	End of simulation 1	Middle Fork	3.31%	P-lapse rate =0.0001, T-lapse rate=variable6, K _L soil8=0.005, soild5,
48	2005	End of simulation 1	Middle Fork	0.55%	P-lapse rate =0.0001, T-lapse rate=variable5, K _L soil8=0.005, soild5, snow threshold =5.0,
49	2005	End of simulation 1	Middle Fork	1.27%	P-lapse rate =0.0001, T-lapse rate=variable3, K _L soil8=0.005, soild5, snow threshold =5.0,
50	2005	End of simulation 1	Middle Fork	0.41%	P-lapse rate =0.0001, T-lapse rate=variable2, K _L soil8=0.005, soild5, snow threshold =5.0,
51	2005	End of simulation 1	Middle Fork	0.66%	P-lapse rate =0.0001, T-lapse rate=variable7, K _L soil8=0.005, soild5, snow threshold =5.0,
52	2005	End of simulation 1	Middle Fork	44.99%	P-lapse rate =0.0012, T-lapse rate=variable7, K _L soil8=0.005, soild5, snow threshold =5.0,
53	2005	End of simulation 1	Middle Fork	1.01%	P-lapse rate =0.0001, T-lapse rate=variable7, K _L soil8=0.005, soild5, snow threshold =5.0, Ice
54	2005	End of simulation 1	Middle Fork	1.13%	P-lapse rate =0.0001, T-lapse rate=variable8, K _L soil8=0.005, soild5, snow threshold =5.0, glacier
55	2005	End of simulation 1	Middle Fork	1.9%	P-lapse rate =0.0001, T-lapse rate=variable8, K _L soil8=0.005, soild5, snow threshold =4.0, Ice
56	2004-05	End of simulation 1	Middle Fork	1.82%	P-lapse rate =0.0001, T-lapse rate=variable8, K _L soil8=0.005, soild5, snow threshold =4.0, Ice

Table B3: Simulations performed using only Middle Fork SNOTEL station. Simulations 55 and 56 are the final calibration and validation simulations (Continued from above).

Appendix C: Contents of Disc

Sample input file

input.mfork

Middle Fork basin GIS:

Digital Elevation Model

Vegetation

Soil Classifications

Soil thickness

Stream network

Watershed boundary

Glaciers

Meteorological Input Files

Middle Fork SNOTEL

Wells Creek

Elbow Lake

Other

Middle Fork streamflow records

AML Files

Compiled C code for shadow maps

Thesis in pdf format